Journal of Enzyme Inhibition and Medicinal Chemistry, 2010; 25(2): 250–265

informa
healthcare

RESEARCH ARTICLE

Human polymerase α inhibitors for skin tumors. Part 2. Modeling, synthesis and influence on normal and transformed keratinocytes of new thymidine and purine derivatives

Monika Höltje[1], Anja Richartz[2], Barbara Zdrazil[1], Anja Schwanke[2], Branislav Dugovic[3], Caterina Murruzzu[3], Hans-Ulrich Reißig[3], Hans Christian Korting[4], Burkhard Kleuser[2], Hans-Dieter Höltje[1], and Monika Schäfer-Korting[2]

[1]Institut für Pharmazeutische und Medizinische Chemie, Heinrich Heine-Universität Düsseldorf, Germany, [2]Institut für Pharmazie (Pharmakologie und Toxikologie) der Freien Universität Berlin, Berlin, Germany, [3]Institut für Chemie und Biochemie (Organische Chemie) der Freien Universität Berlin, Berlin, Germany, and [4]Klinik und Poliklinik für Dermatologie und Allergologie der Ludwig-Maximilians-Universität, München, Germany

Abstract

Recently, the three-dimensional structure of the active site of human DNA polymerase α (pol α) was proposed based on the application of molecular modeling methods and molecular dynamic simulations. The modeled structure of the enzyme was used for docking selective inhibitors (nucleotide analogs and the non-nucleoside inhibitor aphidicolin) in its active site in order to design new drugs for actinic keratosis and squamous cell carcinoma (SCC). The resulting complexes explained the geometrical and physicochemical interactions of the inhibitors with the amino acid residues involved in binding to the catalytic site, and offered insight into the experimentally derived binding data. The proposed structures were synthesized and tested *in vitro* for their influence on human keratinocytes and relevant tumor cell lines. Effects were compared to aphidicolin which inhibits pol α in a non-competitive manner, as well as to diclofenac and 5-fluorouracil, both approved for therapy of actinic keratosis. Here we describe three new nucleoside analogs inhibiting keratinocyte proliferation by inhibiting DNA synthesis and inducing apoptosis and necrosis. Thus, the combination of modeling studies and *in vitro* tests should allow the derivation of new drug candidates for the therapy of skin tumors, given that the agents are not relevant substrates of nucleotide transporters expressed by skin cancer cells. Kinases for nucleoside activation were detected, too, corresponding with the observed effects of nucleoside analogs.

Keywords: *Human DNA polymerase; polymerase inhibitors; keratinocytes; molecular dynamic simulations; nucleoside analogs; kinases; nucleoside transporters*

Abbreviations: 5-FU, 5-fluorouracil; annexin V-FITC, rh annexin V labeled with fluorescein isothiocyanate; ara-G (nelarabine), 2-amino-9-β-D-arabinofuranosyl-6-methoxy-9H-purine; ATCC, American Type Culture Collection; dCK, deoxycytidine kinase; dGK, deoxyguanosine kinase; DMEM, Dulbecco's modified Eagle's medium; DMSO, dimethylsulfoxide; dNTP, deoxynucleoside triphosphate; EDTA, ethylene diamine tetraacetic acid; FCS, fetal calf serum; GAPDH, glyceraldehyde 3-phosphate dehydrogenase; HaCaT, spontaneously transformed human keratinocyte cell line; hENT-1, human equilibrative nucleoside transporter; KBM, keratinocyte basal medium; KGM, keratinocyte growth medium; MCF-7, human breast adenocarcinoma cell line; MRP, multidrug resistance protein; MTT, methylthiazolyldiphenyltetrazolium bromide; NHK, normal human keratinocytes; NRU, neutral red uptake; PBS, phosphate buffered saline, pH 7.4; PI, propidium iodide; RPMI, Roosevelt Park Memorial Institute; RT-PCR, reverse transcriptase polymerase chain reaction; SCC, squamous cell carcinoma; TK-1, thymidine kinase; TPace, thymidine phosphorylase; TP, triphosphate

Address for Correspondence: Prof. Dr. M. Schäfer-Korting, Institut für Pharmazie der Freien Universität Berlin, Königin-Luise-Str. 2-4, D-14195 Berlin, Germany. Tel: +49 30 838 53283. Fax: +49 30 838 54399. E-mail: msk@zedat.fu-berlin.de

(Received 24 November 2008; revised 8 May 2009; accepted 18 May 2009)

ISSN 1475-6366 print/ISSN 1475-6374 online
DOI: 10.3109/14756360903059579

http://www.informahealthcare.com/enz

Introduction

Due to an increased ultraviolet (UV) exposure of Western society, the number of patients with actinic keratosis and cutaneous squamous cell carcinoma is increasing dramatically. Current therapy of actinic keratosis is painful, as with 5-fluorouracil (5-FU)[1] and photodynamic therapy[2], and/or cure rates are not totally satisfying, as with 5-FU, diclofenac/hyaluronic acid[3], and imiquimod[4]. Hence we are looking for alternative approaches, such as interference with DNA synthesis. The human DNA polymerase α (pol α) catalyzes the very first steps in DNA replication and therefore is an interesting target. Recently, selective non-nucleoside inhibitors of pol α such as dehydroaltenusin[5], glycolipids from green tea and spinach, and acyl-catechins[6–9] have been described, strengthening the relevance of this target. In fact, some nucleoside pol α inhibitors are already used systemically for leukemia (cytarabine, fludarabine[10]) and pancreatic carcinoma (gemcitabine). Inhibition of DNA synthesis correlates with the inhibition of pol α activity by gemcitabine and cytarabine triphosphates in the breast cancer cell line MCF-7[11].

To obtain systematic access to the innovative target we modeled the structure of the active site of pol α[12]. Molecular dynamics simulations and docking of a series of known inhibitors into the active site enabled us to validate our 3D model. Moreover, molecular modeling allowed us to identify selective nucleoside inhibitors, which are described here. To test the potential of pol α inhibition in skin cancer, we investigated the influence of the new substances and the known pol α and pol δ inhibitor aphidicolin[13] on keratinocyte proliferation, cell cycle distribution, and cell death. Effects were compared to those of agents used for the therapy of actinic keratosis and antiviral polymerase inhibitors, which served as the negative control. Since therapeutic failure with nucleoside analogs can result from a lack of enzymatic activation by kinases, degradation by phosphorylases, or inducible drug transport out of the tumor cell, we also tested keratinocytes for mRNA expression of relevant enzymes and transporters.

Materials and methods

Molecular modeling

Molecular modeling methods, as well as the design and properties of the pol α active site model, have been described in detail previously, and will not be discussed here[12]. Triphosphates (TPs) of BuP-OH (**2a**), iso-Hex-OH (**2b**), and HM-1 (**1**) (Scheme 1) were docked manually into the active site, and the resulting interaction complexes were minimized. As a confirmation of this procedure, molecular dynamics simulations were performed to investigate the stability of the active site–inhibitor complexes.

Synthesis

The starting materials 3-acetylaminophenyl butanoate (**5a**), *N*-(4-butyryl-3-hydroxyphenyl)acetamide[14] (**6a**), 2-deoxy-3,5-di-*p*-tolyl-D-ribofuranosyl chloride[15] (**11**), and 5′-O-(4,4′-dimethoxytrityl)thymidine[16] (**14**) were prepared according to literature procedures. All other chemicals were commercially available and were used without further purification. The solvents were dried using standard procedures. Products were purified by flash column liquid chromatography (FLC) on silica gel (230–400 mesh; Merck, Darmstadt, Germany). Thin layer chromatography (TLC) was performed on pre-coated silica gel plates $60F_{254}$ and visualized with a UV lamp (254 nm) or using a solution of $KMnO_4/Na_2CO_3$ in water followed by heating. Preparative high performance liquid chromatography (HPLC) was carried out on a Nucleosil 50-5 column and detected with a Knauer variable UV detector (λ = 254 nm, Smartline UV Detector 2600) and a Knauer refractometer (Smartline RI Detector 2400; Knauer, Berlin, Germany). Unless stated otherwise, yields refer to analytically pure samples. ^1H and ^{13}C nuclear magnetic resonance (NMR) spectra were recorded on Jeol Eclipse 500 (500 MHz; Jeol, Tokyo, Japan) and Bruker AC 250 (250 MHz; Bruker, Karlsruhe, Germany) instruments. Infrared (IR) spectra were measured with a Fourier transform (FTIR) spectrometer Nicolet 5 SXC, and a Nicolet 5 SX205 (PerkinElmer, Rodgau-Jügesheim, Germany). Mass spectrometry (MS) and high resolution mass spectrometry (HRMS) analyses were performed on Finnigan (Bremen, Germany) MAT 711 (electron ionization (EI), 80 eV, 8 kV) and MAT CH7A (EI, 80 eV, 3 kV) instruments. Elemental analyses were recorded with a Vario EL analyzer (Elementar Analysensysteme GmbH, Hanau, Germany). Optical rotations ($[\alpha]_D$) were determined with a PerkinElmer 141 or PerkinElmer 241 polarimeter at the temperature given.

Synthesis of compound 1

5′-O-(4,4′-Dimethoxytrityl)-3′-ketothymidine (15). A suspension of **14** (1.67 g, 3.06 mmol) in CH_2Cl_2 (25 mL) was added to a suspension of Dess–Martin reagent (1.95 g, 4.60 mmol) in CH_2Cl_2 (25 mL) at 0°C. After 15 min the temperature was allowed to warm up to room temperature and the mixture was stirred for 6 h. The solution was diluted with Et_2O (100 mL), poured into 60 mL of ice-cold saturated $NaHCO_3/H_2O$ containing $Na_2S_2O_3 \cdot 5H_2O$ (7.70 g), and shaken for 5 min in an ice bath. The organic phase was separated, washed with saturated $NaHCO_3$ solution, H_2O, and brine, dried with Na_2SO_4, and concentrated under vacuum to give a colorless foam (1.76 g quant., purity ca. 95% according to ^1H

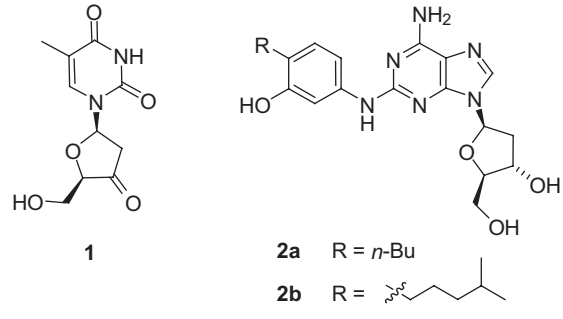

Scheme 1. Structures of polymerase α (pol α) inhibitors designed by molecular modeling: **1**, HM-1; **2a**, BuP-OH; **2b**, iso-Hex-OH.

NMR spectroscopy). The crude product was used for further steps without purification. ^{1}H NMR (500 MHz, $CDCl_3$) δ 8.82 (s, 1H), 7.66 (d, *J* = 1.3 Hz, 1H), 7.35–7.33 (m, 2H), 7.30–7.22 (m, 7H), 6.84–6.81 (m, 4H), 6.58 (dd, *J* = 8.2, 6.7 Hz, 1H), 4.17 (t, *J* = 2.3 Hz, 1H), 3.79 (s, 6H), 3.64 (dd, *J* = 10.4, 2.3 Hz, 1H), 3.43 (dd, *J* = 10.4, 2.3 Hz, 1H), 3.08 (dd, *J* = 18.6, 6.7 Hz, 1H), 2.75 (dd, *J* = 18.6, 8.2 Hz, 1H), 1.32 (d, *J* = 1.3 Hz, 3H) ppm. ^{13}C NMR (125 MHz, $CDCl_3$) δ 209.5, 163.4, 158.8, 150.3, 144.1, 135.1, 134.9, 134.8, 130.0, 128.0, 127.2, 113.3, 112.4, 87.1, 81.5, 80.9, 63.0, 55.2, 41.9, 11.4 ppm.

3′-Ketothymidine (1). To a solution of **15** (1.00 g, 1.84 mmol) in CH_2Cl_2 (5 mL) at 0°C, 2% trifluoroacetic acid (TFA) in CH_2Cl_2 (25 mL) was added drop-wise. After 15 min the solvent was removed under vacuum (bath temperature was kept at 25°C) and the orange residue was three-times co-evaporated with CH_2Cl_2. Another portion of cold CH_2Cl_2 was added and the resulting solid was filtered and washed with cold CH_2Cl_2 to give **1** (0.30 g, 69%) as a pink solid (purity ca. 95% according to ^{1}H NMR), mp 198–200°C. $[\alpha]_D^{23}$ = +108.4 (*c* = 0.51, DMSO). IR (KBr): *ν* 3425, 3240, 1755, 1715, 1665 cm^{-1}. ^{1}H NMR (500 MHz, DMSO-d_6) δ 11.36 (s, 1H), 7.81 (d, *J* = 1.2 Hz, 1H), 6.39 (t, *J* = 7.1 Hz, 1H), 5.15 (br, 1H), 4.10 (t, *J* = 3.2 Hz, 1H), 3.67 (d, *J* = 3.3 Hz, 2H), 2.91 (dd, *J* = 18.6, 7.1 Hz, 1H), 2.67 (dd, *J* = 18.6, 7.1 Hz, 1H), 1.78 (d, *J* = 1.2 Hz, 3H) ppm. ^{13}C NMR (125 MHz, DMSO-d_6) δ 211.1, 163.9, 150.8, 137.2, 109.8, 83.0, 81.7, 61.1, 40.9, 12.4 ppm. MS (FAB): *m/z* (%) 263 (5) [M$^+$ + Na], 241 (7) [M$^+$ + H].

Synthesis of compound 2a

N-(4-Butyl-3-hydroxyphenyl)acetamide. A flask containing ketone **6a** (5.00 g, 22.6 mmol), Pd–C (1.37 g, 1.29 mmol, 10% Pd), methanesulfonic acid (1.75 mL, 27.0 mmol), acetic acid (4.75 mL), EtOAc (165 mL), and EtOH (165 mL) was thoroughly purged with argon and then hydrogen. The reaction mixture was stirred under an atmosphere of hydrogen until the ketone spot disappeared on TLC. The mixture was filtered through a Celite pad, which was subsequently washed with EtOAc (600 mL). The residue was taken up in 150 mL of EtOAc and treated for 1 h with saturated $NaHCO_3$ solution (150 mL). The phases were separated and the aqueous layer was extracted with EtOAc (3 × 100 mL). The organic layer was dried with Na_2SO_4 and concentrated under vacuum. The crude product was purified by flash chromatography on silica gel (CH_2Cl_2/MeOH, 96:4). The product (4.04 g, 86%) was obtained as a brownish solid, mp 143–148°C. Retention factor (R_f) = 0.25 (CH_2Cl_2/MeOH, 96:4). The spectroscopic data are in accordance with those published.

N-(3-Benzyloxy-4-butylphenyl)acetamide. Benzylbromide (2.6 mL, 22.0 mmol) was added to a mixture of the obtained phenol (4.00 g, 19.3 mmol) and K_2CO_3 (6.25 g, 45.2 mmol) in dry acetone (75 mL). The mixture was heated at reflux overnight and then filtered through a Celite pad, which was subsequently washed with acetone. The solvent was removed under vacuum and the residue was treated with hexane (100 mL). The resulting precipitate was collected to give the benzyl ether (4.51 g, 79%) as a colorless solid, mp 73–75°C. R_f = 0.57 (CH_2Cl_2/MeOH, 96:4). IR (KBr): *ν* 3330, 3310, 3270, 1660, 1550 cm^{-1}. ^{1}H NMR (500 MHz, $CDCl_3$): δ 7.52 (br s, 1H), 7.41–7.40 (m, 3H), 7.38–7.35 (m, 2H), 7.31–7.28 (m, 1H), 7.04 (d, *J* = 8.1 Hz, 1H), 6.82 (dd, *J* = 8.1, 1.9 Hz, 1H), 5.03 (s, 2H), 2.61 (t, *J* = 7.6 Hz, 2H), 2.13 (s, 3H), 1.58–1.52 (m, 2H), 1.34 (sext., *J* = 7.4 Hz, 2H), 0.90 (t, *J* = 7.4 Hz, 3H). ^{13}C NMR (125 MHz, $CDCl_3$): δ 168.4, 156.7, 137.3, 136.8, 129.7, 128.4, 127.7, 127.6, 127.0, 111.6, 104.3, 69.7, 32.1, 29.6, 24.5, 22.5, 13.9. MS (EI): *m/z* (%) 297 (16) [M$^+$], 254 (8) [M$^+$ – C_2H_3O], 91 (100) [C_7H_7]$^+$. HRMS (EI) calcd for $C_{19}H_{23}NO_2$ 297.1729, found 297.1733.

*3-Benzyloxy-4-butylphenylamine (**7a**).* Claisen's alkali was prepared by dissolving KOH (17.4 g, 310 mmol) in 12.5 mL of water. After cooling, 50 mL of MeOH was added. The acetamide derivative (4.40 g, 14.8 mmol) was refluxed for 4 h in 50 mL of Claisen's alkali solution. The cooled solution was diluted with 200 mL of water and 100 mL of EtOAc. The resulting mixture was extracted with EtOAc (3 × 50 mL). The combined organic layers were dried with Na_2SO_4 and concentrated under vacuum. The pure product **7a** (3.56 g, 94%) was obtained by Kugelrohr distillation (250°C, 0.25 mbar) as a slightly yellowish oil. R_f = 0.88 (CH_2Cl_2/MeOH, 96:4). IR (KBr): *ν* 3435, 3355, 1620 cm^{-1}. ^{1}H NMR (500 MHz, $CDCl_3$): δ 7.43–7.41 (m, 2H), 7.39–7.36 (m, 2H), 7.32–7.29 (m, 1H), 6.92 (d, *J* = 8.0 Hz, 1H), 6.27 (d, *J* = 2.2 Hz, 1H), 6.24 (dd, *J* = 8.0, 2.2 Hz, 1H), 5.01 (s, 2H), 3.53 (br s, 2H), 2.56 (t, *J* = 7.7 Hz, 2H), 1.58–1.51 (m, 2H), 1.34 (sext., *J* = 7.4 Hz, 2H), 0.90 (t, *J* = 7.4 Hz, 3H). ^{13}C NMR (125 MHz, $CDCl_3$): δ 157.3, 145.4, 137.6, 130.4, 128.4, 127.6, 126.9, 121.9, 107.2, 100.0, 69.7, 32.5, 29.3, 22.5, 14.0. MS (EI): *m/z* (%) 255 (22) [M$^+$], 212 (30) [M$^+$ – C_3H_7], 164 (5) [M$^+$ – C_7H_3], 91 (100) [C_7H_7]$^+$. HRMS (EI) calcd for $C_{17}H_{21}NO$ 255.1623, found 255.1626. Anal. $C_{17}H_{21}NO$: calcd C, 79.96; H, 8.29; N, 5.49. Found: C, 80.97; H, 8.13; N; 5.68%.

*N2-(3-Benzyloxy-4-butylphenyl)guanine (**9a**).* A solution of 2-bromohypoxanthine **8** (0.80 g, 3.72 mmol) and aniline derivative **7a** (2.85 g, 11.2 mmol) in a mixture of 2-methoxyethanol (24 mL) and water (8 mL) was heated at reflux until the spot of 2-bromohypoxanthine disappeared on TLC (5 h). The mixture was cooled; the fine precipitate formed was filtered, and washed with saturated aqueous ammonia (5 mL) and cold MeOH (3 × 5 mL). The slightly yellowish sticky solid was triturated with MeOH (3 × 5 mL) to give product **9a** (1.31 g, 90%) as a fine colorless powder, mp 306–307°C. IR (KBr) *ν* = 1700 cm^{-1}. ^{1}H NMR (500 MHz, DMSO-d_6): δ 13.11, 12.69 (2 × br s, 1H), 10.52 (br s, 1H), 8.66, 8.52 (2 × br s, 1H), 8.03, 7.78 (2 × br s, 1H), 7.50–7.30 (m, 6H), 7.07 (s, 2H), 5.12 (s, 2H), 2.55 (t, *J* = 7.4 Hz, 2H), 1.51 (quint., *J* = 7.4 Hz, 2H), 1.28 (sext., *J* = 7.4 Hz, 2H), 0.86 (t, *J* = 7.4 Hz, 3H). ^{13}C NMR (125 MHz, DMSO-d_6): δ 156.2, 137.3, 129.7, 128.5, 127.8, 127.5, 69.3, 31.8, 29.0, 22.0, 13.8. MS (EI): *m/z* (%) 389 (8) [M$^+$], 347 (23) [M$^+$ – C_3H_6], 298 (4) [M$^+$ – C_7H_7], 91 (100) [C_7H_7]$^+$. Anal. $C_{22}H_{23}N_5O_2$: calcd C, 67.85; H, 5.95; N, 17.98. Found: C, 67.91; H, 5.84; N; 18.41%.

*2-(3-Benzyloxy-4-butylphenylanilino)-6-chloropurine (**10a**)*

A solution of **9a** (0.77 g, 1.97 mmol) in $POCl_3$ (5.5 mL, 60.0 mmol) containing *N,N*-dimethylaniline (0.63 mL, 4.94 mmol) was heated at reflux for 10 min. The reaction

mixture was poured slowly into an ice-water solution and after 2 h it was brought to pH 3 with AcONa. The yellow solid was collected by filtration, then it was dissolved in MeOH and filtered through a Celite pad. Compound **10a** was obtained (0.75 g, 94%) as a brownish solid, mp 109–110°C, and was used for the next step without further purification. R_f = 0.64 (CH_2Cl_2/MeOH, 98:2). IR (KBr): ν 1630, 1570 cm^{-1}. ^1H NMR (500 MHz, CD_3OD): δ 8.15 (s, ^1H), 7.62 (d, *J* = 2.0 Hz, 1H), 7.50 (d, *J* = 7.1 Hz, 2H), 7.40–7.37 (m, 2H), 7.33–7.31 (m, 1H), 7.18 (dd, *J* = 8.1, 2.0 Hz, 1H), 7.02 (d, *J* = 8.1 Hz, 1H), 5.12 (s, 2H), 2.61 (t, *J* = 7.4 Hz, 2H), 1.58 (quint., *J* = 7.4 Hz, 2H), 1.37 (sext., *J* = 7.4 Hz, 2H), 0.93 (t, *J* = 7.4 Hz, 3H). ^{13}C NMR (125 MHz, CD_3OD): δ 158.2, 158.0, 143.7, 140.6, 139.3, 130.9, 129.7, 129.0, 128.8, 126.6, 112.6, 105.0, 71.3, 33.9, 31.0, 23.9, 14.7. MS (EI): *m/z* (%) 407 (31) [M^+], 364 (45), 316 (11) [M^+ – C_7H_7], 91 (100) [$C_7H_7]^+$.

2-(3-Benzyloxy-4-butylphenylanilino)-6-chloro-9-(2-deoxy-3,5-di-p-toluyl-β-D-ribofuranosyl)purine (12a). To a suspension of **10a** (0.75 g, 1.85 mmol) in MeCN (15 mL), NaH (50% suspension in mineral oil, 0.09 g, 2.0 mmol) was added. After 45 min the chloride **11** (0.75 g, 2.08 mmol) was added in small portions during 30 min and the solution was stirred at room temperature for 1.5 h. The mixture was diluted with CH_2Cl_2 (10 mL), filtered through Celite, and concentrated under vacuum. Purification by flash chromatography on silica gel (EtOAc/hexane, 25:75 to 35:65) gave the desired product **12a** (0.71 g, 51%) as white foam, mp 70–73°C. $[\alpha]_D^{23}$ = –6.1 (*c* = 1.09; $CHCl_3$). R_f = 0.43 (EtOAc/hexane, 1:1). IR (KBr): ν 3390–2860, 1720 cm^{-1}. ^1H NMR (500 MHz, $CDCl_3$): δ 7.95 (s, 1H), 7.93 (d, *J* = 8.2 Hz, 2H), 7.86 (d, *J* = 8.2 Hz, 2H), 7.43–7.29 (m, 7H), 7.25 (d, *J* = 8.0 Hz, 2H), 7.19 (d, *J* = 8.0 Hz, 2H), 7.12 (dd, *J* = 8.1, 1.9 Hz, 1H), 7.10 (d, *J* = 8.1 Hz, 1H), 6.44 (dd, *J* = 7.8, 6.0 Hz, 1H), 5.76 (dt, *J* = 6.0, 2.2 Hz, 1H), 5.12 (s, 2H), 4.79 (dd, *J* = 13.1, 5.7 Hz, 1H), 4.64–4.60 (m, 2H), 3.11 (ddd, *J* = 14.2, 7.8, 6.0 Hz, 1H), 2.78 (ddd, *J* = 14.2, 6.0, 2.2 Hz, 2H), 2.62 (t, *J* = 7.4 Hz, 2H), 2.44, 2.38 (2 × s, 2 × 3H), 1.57 (quint., *J* = 7.4 Hz, 2H), 1.36 (sext., *J* = 7.4 Hz, 2H), 0.91 (t, *J* = 7.4 Hz, 3H). ^{13}C NMR (125 MHz, $CDCl_3$): δ 166.2, 165.8, 156.7, 155.7, 152.5, 151.2, 144.5, 144.2, 140.5, 137.7, 137.3, 129.9, 129.7, 129.5, 129.3, 129.2, 128.4, 127.7, 127.0, 126.8, 126.7, 126.5, 126.3, 111.6, 104.0, 84.8, 82.9, 75.0, 69.8, 63.7, 37.5, 32.2, 29.5, 22.6, 21.7, 21.7, 14.0. MS (EI): *m/z* (%) 759 (100) [M^+], 716 (3) [M^+ – C_3H_7], 119 (85) [$C_8H_7O]^+$, 91 (81) [$C_7H_7]^+$. HRMS (EI) calcd for $C_{43}H_{42}ClN_5O_6$ 759.2823, found 759.2866.

2-(3-Benzyloxy-4-butylphenylanilino)-6-azido-9-(2-deoxy-β-D-ribofuranosyl)purine (13a). A mixture of **12a** (0.40 g, 0.53 mmol) and NaN_3 (0.34 g, 5.31 mmol) in dimethylformamide (DMF) (10 mL) was heated at 60°C for 4.75 h. The solution was then diluted with EtOAc (10 mL), filtered through Celite, and concentrated under vacuum. The residue was purified by flash chromatography on silica gel (EtOAc/hexane, 1:1) to give 0.47 g of a yellow honey, which was dissolved in MeOH (13 mL). The resulting solution was treated with a solution of 0.5 N MeONa in MeOH (2.12 mL, 1.06 mmol) for 24 h. The solvent was removed under vacuum and the residue was filtered through silica gel (EtOAc/hexane/MeOH, 5:5:1). The crude product **13a** (0.20 g, 69%) was obtained as a dark-yellow honey and used without further purification to the next step. R_f = 0.30 (EtOAc/hexane/MeOH, 5:5:1).

2-(4-Butyl-3-hydroxyphenylanilino)-2'-deoxyadenosine (2a). Argon was passed through the mixture of **13a** (0.20 g, 0.39 mmol) and 5% HCOOH in MeOH (15 mL) for 10 min. Pd-black (0.09 g, 0.81 mmol) was added and the mixture was stirred under a hydrogen atmosphere at room temperature for 23 h. The reaction mixture was filtered through Celite and concentrated under vacuum. Purification by flash chromatography on silica gel (EtOAc/hexane/MeOH, 5:5:1) gave **2a** (0.11 g, 68%) as a brownish solid, mp 113–115°C. $[\alpha]_D^{23}$ = +15.0 (*c* = 1.02; MeOH). R_f = 0.47 (CH_2Cl_2/MeOH, 9:1). IR (KBr): ν 3390–2860, 1635 cm^{-1}. 1H NMR (500 MHz, CD_3OD): δ 8.09 (s, 1H), 7.40 (d, *J* = 2.0 Hz, ^1H), 6.97 (d, *J* = 8.1 Hz, 1H), 6.91 (dd, *J* = 8.1, 2.0 Hz, 1H), 6.45 (dd, *J* = 7.3, 6.5 Hz, 1H), 4.61 (dt, *J* = 6.2, 3.0 Hz, 1H), 4.06 (ddd, *J* = 4.0, 3.5, 3.0 Hz, 1H), 3.84 (dd, *J* = 12.1, 3.5 Hz, 1H), 3.77 (dd, *J* = 12.1, 4.0 Hz, 1H), 2.87 (ddd, *J* = 13.5, 7.3, 6.2 Hz, 1H), 2.58 (t, *J* = 7.5 Hz, 2H), 2.44 (ddd, *J* = 13.5, 6.5, 3.0 Hz, 1H), 1.59 (quint., *J* = 7.5 Hz, 2H), 1.41 (sext., *J* = 7.5 Hz, 2H), 0.98 (t, *J* = 7.5 Hz, 3H). ^{13}C NMR (125 MHz, CD_3OD): δ 158.4, 157.4, 156.2, 152.1, 140.7, 138.7, 130.8, 123.9, 115.3, 111.9, 107.7, 89.2, 85.9, 72.9, 63.5, 41.1, 33.6, 30.5, 23.6, 14.5. MS (FAB): *m/z* (%) 437 (<1) [M^+ + Na], 415 (6) [M^+ + H], 414 (4) [M^+].

Synthesis of compound 2b

4-Methylpentanoyl chloride (4b). 4-Methylvaleric acid (5.00 g, 43.1 mmol) was dissolved in $CHCl_3$ (30 mL) and thionyl chloride (4.70 mL, 64.6 mmol) was added drop-wise. The mixture was heated to 80°C for 2 h. The excess of $SOCl_2$ and solvent were removed by distillation (atmospheric pressure, 140°C) and pure product **4b** was obtained as a yellow liquid (5.20 g, 90%). ^1H NMR (250 MHz, $CDCl_3$): δ 2.86 (mc, 2H), 1.58 (mc, 3H), 0.90 (d, *J* = 5.7 Hz, 6H). ^{13}C NMR (125 MHz, $CDCl_3$): δ 173.9, 42.3, 33.6, 21.9, 22.1.

3-Acetamidophenyl 4-methylpentanoate (5b). To a suspension of 3-acetamidophenol **3** (5.00 g, 30.4 mmol) in dry toluene (50 mL) were added pyridine (0.05 mL) and acid chloride **4b** (4.50 g, 33.4 mmol). The mixture was heated to 95°C for 1 h, then an additional 0.5 mL of **4b** was added and the heating continued for 30 min. The cooled mixture was poured into ice and extracted with Et_2O (3 × 20 mL). The combined organic phases were washed with 0.5 M HCl and a saturated $NaHCO_3$ solution and dried with $MgSO_4$. The solvents were removed and the crude product was purified by flash chromatography on silica gel (hexane/EtOAc, 7:3). Product **5b** was obtained as a red oil (5.30 g, 70%). IR (film): ν 3300, 2960, 1755, 1670, 1605 cm^{-1}. ^1H NMR (500 MHz, $CDCl_3$): δ 8.21 (s, 1H), 7.42 (mc, 2H), 7.23 (mc, 1H), 6.72 (dd, *J* = 8.0, 2.1 Hz, 1H), 2.56 (t, *J* = 7.3 Hz, 2H), 2.03 (s, 3H), 1.64 (mc, 3H), 0.94 (d, *J* = 6.8 Hz, 6H). ^{13}C NMR (125 MHz, $CDCl_3$): δ 173.1, 168.9, 150.8, 139.3, 128.9, 116.9, 116.7, 113.3, 33.5, 32.4, 27.6, 24.2, 22.2. HRMS (*m/z*) calcd for $C_{14}H_{20}NO_3$ $[MH]^+$ 250.1365, found 250.1432.

N-[4-(4-Methylpentanoyl)-3-hydroxyphenyl) acetamide (6b). Compound **5b** (6.50 g, 26.1 mmol) and $AlCl_3$ (12.2 g,

91.3 mmol) were sealed in a dry round-bottomed flask and shaken vigorously for 5 min. The flask was connected to a condenser fitted to a bubbler and a gas absorption tube (NaOH solution), and the mixture was slowly heated to 130°C for 3 h. To the cooled mixture, ice was added (50 g) followed by the addition of 2 N H_2SO_4 (50 mL), and the mixture was stirred overnight at room temperature. The brownish solid was filtered, and washed with water and dry toluene. Recrystallization from 50 mL of toluene gave product **6b** (4.55 g, 75%) as a yellow solid; mp 78–80°C. IR (KBr): ν 3300, 2955, 1675, 1625, 1545 cm^{-1}. ^1H NMR (500 MHz, $CDCl_3$): δ 12.63 (s, 1H), 8.06 (s, 1H), 7.68 (d, *J* = 8.7 Hz, 1H), 7.16 (d, *J* = 8.7 Hz, 1H), 7.09 (s, 1H), 2.89 (t, *J* = 7.3 Hz, 2H), 2.18 (s, 3H), 1.61 (mc, 3H), 0.89 (d, *J* = 6.6 Hz, 6H). ^{13}C NMR (125 MHz, $CDCl_3$): δ 205.9, 169.2, 163.9, 144.9, 131.4, 115.8, 110.4, 107.5, 36.2, 33.7, 27.9, 24.8, 22.4. HRMS (*m/z*) calcd for $C_{14}H_{20}NO_3$ $[MH]^+$ 250.1365, found 250.1432.

N-(4-(4-Methylpentyl)-3-hydroxyphenyl) acetamide. A flask containing compound **6b** (2.00 g, 8.10 mmol), Pd–C (0.84 g, 0.80 mmol), methanesulfonic acid (0.60 mL, 9.61 mmol), acetic acid (1.70 mL), EtOAc (55 mL), and EtOH (55 mL) was first purged with argon and then with hydrogen. The mixture was stirred under an atmosphere of hydrogen until the ketone spot disappeared on TLC. The mixture was filtered through a Celite pad which was subsequently washed with EtOAc. The residue was dissolved in EtOAc (75 mL) and treated for 1 h with saturated $NaHCO_3$ solution (75 mL). The phases were separated and the aqueous layer was extracted with EtOAc (3 × 20 mL). The combined organic layers were dried with Na_2CO_3 and concentrated under vacuum. The crude product was purified by flash chromatography on silica gel (CH_2Cl_2/MeOH, 96:4) and the product was obtained as a brownish solid (1.62 g, 85%); mp 80–82°C. IR (KBr): ν 3395, 3180, 2955, 1650, 1420 cm^{-1}. ^1H NMR (500 MHz, CD_3OD): δ 7.18 (d, *J* = 2 Hz, 1H), 6.98 (d, *J* = 8.1 Hz, 1H), 6.80 (dd, *J* = 8.1, 2.0 Hz, 1H), 2.53 (t, *J* = 7.8 Hz, 2H), 2.08 (s, 3H), 1.55 (mc, 3H), 1.22 (mc, 2H) 0.89 (d, *J* = 6.6 Hz, 6H). ^{13}C NMR (125 MHz, CD_3OD): δ 171.4, 156.3, 138.3, 130.8, 126.5, 112.3, 108.4, 39.9, 31.0, 29.0, 23.7, 23.0, 14.4. HRMS (*m/z*) calcd for $C_{14}H_{21}NO_2$ $[M]^+$ 236.1645, found 236.1642.

N-(3-Benzyloxy-4-(4-methylpentyl)phenyl) acetamide. The precursor phenol derivative (2.00 g, 8.46 mmol) was dissolved in dry acetone (30 mL) and K_2CO_3 (2.70 g, 19.5 mmol) was added. After 20 min, benzyl bromide (1.10 mL, 9.30 mmol) was added and the mixture was refluxed overnight. The solution was filtered through a Celite pad and the solvent was removed under vacuum. The residue was treated with hexane (50 mL) and the resulting precipitate was filtered to give the benzyl ether (1.60 g, 65%) as a colorless solid; mp 98–100°C. IR (KBr): ν 3225, 2955, 1660, 1615, 1550 cm^{-1}. ^1H NMR (500 MHz, $CDCl_3$): δ 7.42 (mc, 4H), 7.35 (t, *J* = 7.7 Hz, 1H), 7.30 (t, *J* = 7.4 Hz, 1H), 7.05 (d, *J* = 7.9 Hz, 1H), 6.82 (dd, *J* = 8.0, 1.8 Hz, 1H), 5.04 (s, 2H), 2.60 (t, *J* = 7.5 Hz, 2H), 2.14 (s, 3H), 1.56 (mc, 3H), 1.23 (mc, 2H) 0.85 (d, *J* = 6.6 Hz, 6H). ^{13}C NMR (125 MHz, $CDCl_3$): δ 168.3, 156.7, 137.3, 136.7, 129.6, 128.5, 127.8, 127.7, 127.2, 111.5, 104, 69.7, 38.9, 30.3, 27.9, 24.7, 22.7. HRMS (*m/z*) calcd for $C_{21}H_{28}NO_2$ $[MH]^+$ 326.2206, found 326.2107.

3-Benzyloxy-4-(4-methylpentyl)phenylamine (7b). To the precursor acetamide (1.50 g, 4.61 mmol), Claisen's alkali solution (4.70 g of KOH, 3.5 mL of H_2O, and 15 mL of MeOH) was added. The mixture was refluxed for 5 h and after cooling diluted with H_2O (50 mL) and EtOAc (70 mL). The resulting mixture was extracted with EtOAc (3 × 20 mL). The combined organic layers were dried with Na_2SO_4 and concentrated. Purification by column using CH_2Cl_2/MeOH (9:1) gave product **7b** as a brownish oil (1.16 g, 89%). IR (KBr): ν 3355, 2950, 1620, 1510, 1445 cm^{-1}. ^1H NMR (500 MHz, $CDCl_3$): δ 7.44 (d, *J* = 6.7 Hz, 1H), 7.39 (t, *J* = 7.2 Hz, 2H), 7.32 (t, *J* = 5.1 Hz, 2H), 6.96 (d, *J* = 7.8 Hz, 1H), 6.38 (d, *J* = 2.2 Hz, 1H), 6.26 (dd, *J* = 7.8, 2.2 Hz, 1H), 5.04 (s, 2H), 3.55 (s, 2H), 2.58 (t, *J* = 7.8 Hz, 2H), 1.61 (mc, 3H), 1.24 (mc, 2H), 0.85 (d, *J* = 6.6 Hz, 6H). ^{13}C NMR (125 MHz, $CDCl_3$): δ 157.3, 145.5, 137.7, 130.4, 130.3, 128.4, 127.6, 126.9, 121.9, 107.3, 100.1, 69.7, 38.9, 29.9, 28.1, 27.8, 22.6. MS (EI): *m/z* (%) 283 (14) $[M]^+$, 212 (25), 91 (100). HRMS calcd for $C_{19}H_{25}NO$ $[MH]^+$ 283.1936, found 283.1924.

N^2-(3-Benzyloxy-4-(4-methylpentyl)phenyl)guanine (9b). A solution of 2-bromohypoxanthine **8** (0.34 g, 1.60 mmol) and aniline derivative **7b** (1.30 g, 4.60 mmol) in a mixture of 2-methoxyethanol (10 mL) and water (2 mL) was heated at reflux until the spot of **8** disappeared on TLC (5 h). After cooling, the fine precipitate formed was filtered, and washed with saturated aqueous ammonia (5 mL) and cold MeOH (3 × 5 mL). The resulting solid was triturated with MeOH (3 × 5 mL) to give **9b** as a yellow solid (0.54 g, 81%); mp 107–109°C. IR (KBr): ν 3040, 2950, 1700, 1595, 1510 cm^{-1}. ^1H NMR (500 MHz, DMSO-d_6): δ 13.20, 12.70 (2 br s, 1H), 10.32 (br s, 1H), 8.65 (br s, 1H), 7.70 (s, 1H), 7.43–7.12 (m, 7H), 6.95 (s, 1H), 5.04 (s, 2H), 2.58 (t, *J* = 7.5 Hz, 2H), 1.54 (mc, 3H), 1.20 (mc, 2H), 0.88 (d, *J* = 6.6 Hz, 6H). ^{13}C NMR (125 MHz, DMSO-d_6): δ 156.1, 137.6, 137.3, 129, 128.4, 127.7, 127.4, 124.7, 111.3, 103.8, 69.2, 38.3, 29.6, 27.4, 27.2, 22.5. HRMS calcd for $C_{24}H_{28}N_5O_2$ $[MH]^+$ 418.2237, found 418.2221.

2-[3-Benzyloxy-4-(4-methylpentyl)phenylanilino]-6-chloropurine (10b). A solution of compound **9b** (0.52 g, 1.24 mmol) in $POCl_3$ (3.50 mL) containing *N,N*-dimethylaniline (0.40 mL, 3.10 mmol) was heated at reflux for 10 min. The mixture was poured into an ice-water solution and after 2 h it was brought to pH 3 with NaOAc. The resulting yellow solid was collected by filtration, then dissolved in MeOH and filtered through a Celite pad, which afforded product **10b** as a yellow solid (0.46 g, 85%); mp 84–87°C. IR (KBr): ν 3400, 2950, 1610, 1570, 1530 cm^{-1}. 1H NMR (500 MHz, $CDCl_3$): δ 7.45 (br s, ^1H), 7.35–7.23 (m, 7H), 7.28 (mc, 3H), 7.18 (d, *J* = 1.7 Hz, 1H), 7.09 (d, *J* = 7.9 Hz, 1H), 6.94 (dd, *J* = 7.9, 1.9 Hz, 1H,), 4.98 (s, 2H), 2.59 (t, *J* = 7.7 Hz, 2H), 1.57 (mc, 3H), 1.23 (mc, 2H), 0.85 (d, *J* = 6.6 Hz, 6H). ^{13}C NMR (125 MHz, $CDCl_3$): δ 157.1, 156.2, 137.2, 137.1, 130.3, 128.6, 128.2, 127.8, 127.0, 113.2, 105.5, 69.9, 39.0, 30.3, 27.9, 27.8, 22.7. HRMS calcd for $C_{24}H_{27}ClN_5O$ $[MH]^+$ 436.1899, found 436.1887.

2-[3-Benzyloxy-4-(4-methylpentyl)phenylanilino]-6-chloro-9-(2-deoxy-3,5-di-p-toluyl-β-D-ribofuranosyl)purine (12b). To a suspension of compound **10b** (0.18 g, 0.41

mmol) in dry MeCN (6 mL), NaH (18 mg, 50% suspension, 0.46 mmol) was added and the mixture was stirred at room temperature for 45 min. Compound **11** (0.17 g, 0.47 mmol) was added in small portions over 10 min and the stirring was continued for 2 h. The mixture was diluted with CH_2Cl_2 (5 mL) and filtered through a Celite pad, and the solvents were removed under vacuum. The crude product was purified by flash chromatography on silica gel using hexane/EtOAc (6:4), providing product **12b** as a yellow solid (0.16 g, 50%); mp 68–70°C. IR (KBr): ν 3385, 2955, 1730, 1610, 1540 cm^{-1}. ^1H NMR (500 MHz, $CDCl_3$): δ 7.96 (s, 2H), 7.93 (d, J = 8.0 Hz, 2H), 7.86 (d, J = 8.0 Hz, 2H), 7.43–7.25 (m, 7H), 7.24 (d, J = 8.0 Hz, 2H), 7.17 (d, J = 8.0 Hz, 2H), 7.12 (dd, J = 8.1, 1.9 Hz, 1H), 7.08 (s, 1H), 6.43 (dd, J = 7.9, 6.0 Hz, 1H), 5.76 (mc, 1H), 5.12 (s, 2H), 4.78 (dd, J = 13.0, 6.0 Hz, 1H), 4.61 (mc, 2H), 3.13 (ddd, J = 14.1. 7.8, 6.2 Hz, 1H), 2.76 (ddd, J = 14.1, 6.1, 2.4 Hz, 1H), 2.60 (t, J = 7.6 Hz, 2H), 2.44 (s, 3H), 2.38 (s, 3H), 1.57 (mc, 3H), 1.24 (mc, 2H), 0.85 (d, J = 6.6 Hz, 6H). ^{13}C NMR (125 MHz, $CDCl_3$): δ 166.3, 165.9, 156.7, 155.6, 152.5, 151.1, 144.4, 144.2, 140.5, 137.7, 137.3, 129.7, 129.5, 129.3, 128.4, 127.7, 127.0, 126.5, 126.3, 111.6, 104.0, 84.9, 83.0, 75.1, 69.9, 63.9, 39.0, 37.6, 30.3, 27.97, 27.94, 22.7, 21.8. HRMS: calcd for $C_{45}H_{46}ClN_5O_6$ $[M]^+$ 788.3455, found 788.3224.

2-[3-Benzyloxy-4-(4-methylpentyl)phenylanilino]-6-azido-9-(2-deoxy-β-D-ribofuranosyl)purine (13b). A mixture of **12b** (0.17 g, 0.22 mmol) and NaN_3 (0.14 g, 2.19 mmol) in DMF (5 mL) was heated at 60°C for 5 h. The solution was diluted with EtOAc (5 mL) and filtered through Celite, and the solvents were removed under vacuum. The crude product was purified by flash chromatography on silica gel with hexane/EtOAc (6:4) to give 0.17 g of a yellow honey, which was dissolved in MeOH (8 mL) and 0.5 N MeONa in MeOH (0.9 mL). The resulting mixture was stirred for 24 h at room temperature. The solvent was evaporated and the crude product was filtered through silica gel (hexane/EtOAc/MeOH, 5:5:1) to give **13b** (0.07 g, 59%) as a yellow honey. The crude product **13b** was used in the next step without further purification. The ^1H NMR spectrum (500 MHz, CD_3OD) shows signals for at least two components (**13b** and its cyclized isomer) and the signal cannot be assigned unambiguously.

2-[4-(4-Methylpentyl)-3-hydroxyphenylanilino]-2'-deoxyadenosine (2b). To a solution of crude **13b** (30 mg, 0.054 mmol) under argon in methanol and 5% of HCOOH (2 mL) was added Pd-black (13 mg, 0.08 mmol), and a hydrogen atmosphere was applied for 24 h. The reaction mixture was filtered through Celite and concentrated. The crude product was purified by flash chromatography using CH_2Cl_2/MeOH (9:1) affording **2b** as a pink solid (10 mg, 42%); mp 120–122°C. $[\alpha]^{23}$ = +16.2 (c = 0.9, MeOH). IR (KBr): ν 3380, 2950, 1635, 1600 cm^{-1}. ^1H NMR (500 MHz, CD_3OD): δ 8.05 (s, 1H), 7.35 (d, J = 2.1 Hz, 1H), 6.93 (d, J = 8.0 Hz, 1H), 6.89 (dd, J = 8.1, 2.0 Hz, 1H), 6.40 (t, J = 6.4 Hz, 1H), 4.57 (dt, J = 6.1, 3.0 Hz, 1H), 4.02 (ddd, J = 3.4 Hz, 1H, H-4'), 3.81 (dd, J = 12.0, 3.4 Hz, 1H), 3.72 (dd, J = 12.1, 3.8 Hz, 1H), 2.82 (mc, 1H), 2.52 (t, J = 7.6 Hz, 1H), 2.40 (ddd, J = 13.5, 6.0, 3.1 Hz, 1H), 1.58 (mc, 3H), 1.21 (mc, 2H), 0.98 (d, J = 6.4 Hz, 6H). ^{13}C NMR (125 MHz, CD_3OD): δ 160.8, 159.8, 158.7, 143.2 (2 × s), 141.2, 133.4, 133.3, 126.4, 114.3, 110.1, 91.7, 88.3, 75.4, 65.9, 43.6, 42.5, 33.5, 31.7, 31.6, 22.6. HRMS calcd for $C_{22}H_{31}N_6O_4$ $[M]^+$ 442.2329, found 443.2393.

Biological methods

Chemicals for cell culture testing were purchased from Sigma-Aldrich (Taufkirchen, Germany), Serva Electrophoresis (Heidelberg, Germany; aphidicolin), or VWR (Berlin, Germany). Media for cell culture were purchased from Sigma-Aldrich, or for normal keratinocytes from Cambrex (Landen, Belgium). Primers were synthesized by TibMolbiol (Berlin, Germany). Reagents and kits for RT-PCR were purchased from Rapidozym (Berlin, Germany), New England Biolabs (Frankfurt, Germany), or Invitrogen (Karlsruhe, Germany). Stock solutions (each 10^{-2} M) were prepared by dissolving diclofenac in ethanol (96%), 5-FU in phosphate buffered saline (PBS), and doxorubicin in pure water, while aphidicolin was dissolved in DMSO (2×10^{-2} M). Stock solutions were diluted with the respective solvents to final concentrations of the test agents of 10^{-3} M to 10^{-8} M. In cell culture, maximum concentrations of ethanol and DMSO were 1% and 0.5%, respectively. In all experiments, cells grown in the presence of the respective solvents served as control.

Cell culture

Normal human keratinocytes (NHK) were isolated from foreskin as described previously[17]. Keratinocytes from at least three donors were pooled and cultured in keratinocyte growth medium that was prepared from keratinocyte basal medium (KBM) by the addition of 0.1 ng/mL epidermal growth factor, 5.0 μg/mL insulin, 0.5 μg/mL hydrocortisone, 30 μg/mL bovine pituitary extract, 50 μg/mL gentamicin sulfate, and 50 ng/mL amphotericin B. For all experiments only cells of the second to the fourth passage were used. Medium for SCC-25 cells (ATCC # CRL-1628) was prepared from Ham's F12/DMEM (1:1) by the addition of 15% FCS (Seromed Biochrom, Berlin, Germany), 0.4 μg/mL hydrocortisone, 100 U/mL penicillin, and 100 μg/mL streptomycin. HaCaT cells were a gift from Professor Fusenig (Heidelberg, Germany) and were grown in RPMI 1640 supplemented with 10% FCS, 2 mM L-glutamine, 100 U/mL penicillin, and 100 μg/mL streptomycin. Cells were subcultured twice a week (SCC-25 1:3 to 1:5, HaCaT 1:10) following trypsinization using 0.05% trypsin/0.02% ethylene diamine tetraacetic acid (EDTA).

DNA synthesis

Cells were grown overnight either in 24-well plates (Falcon; Becton Dickinson GmbH, Heidelberg, Germany; 4×10^4 cells per well) or in six-well plates (TPP; 1×10^5 cells per well) in growth medium. Then, the medium was replaced by fresh growth medium adding the indicated agents (10^{-10} M to 10^{-4} M) for 72 h. For the last 23 h cells were pulsed with 1 μCi [^{3}H-methyl]thymidine (Amersham, Buckinghamshire, UK). Cells were washed once with ice-cold PBS and twice with trichloroacetic acid (5%). The precipitated material

was dissolved in 250 µL of 0.3 N NaOH per well and shaken for 1 h/300 rpm. Following thorough mixing with 1.25 mL of OptiPhaseSuperMix scintillation fluid (PerkinElmer, Rodgau-Jügesheim, Germany), incorporated [^{3}H]thymidine was measured by liquid scintillation counting (MicroBeta™ Plus; Wallac, Freiburg, Germany).

MTT dye-reduction assay

Cells (4×10^4 cells per well) were grown in growth medium overnight (24-well plates). Medium was replaced by fresh growth medium for keratinocytes and HaCaT cells or basal medium for SCC-25, respectively. Then the indicated agents were added for 48 h (if not stated otherwise) and MTT solution (final concentration of 0.5 mg/mL) for the last 4 h. After removing supernatants and solubilization of formazan crystals in DMSO, the optical density was determined at 540 nm (Fluostar Optima; BMG Labtech, Offenburg, Germany) as described[18].

Neutral red uptake (NRU)

Cells (4×10^4 cells per well) were grown as described for the MTT assay. The indicated agents were added for 45 h. Medium was replaced by the respective medium containing neutral red at a concentration of 50 µg/mL for another 3 h. After removing the neutral red-containing supernatants, cells were washed with ice-cold PBS. Following the addition of ethanol 50% containing 1% of glacial acetic acid (99%), the optical density was determined at 540 nm as described[19].

Cell cycle distribution

Cells (5×10^4 cells per well) were grown in six-well plates in growth medium overnight and the medium was replaced by fresh growth medium, adding the indicated agents for 48 h. After centrifugation of trypsinized cells, the pellet was dissolved in 0.9 mL PBS and the cells were fixed in 2.1 mL ethanol (96%) for at least 30 min at –20°C and centrifuged again. The cell pellet was washed once with PBS and then dissolved in 200 µL PBS containing PI (40 µg/mL) and RNase A (100 µg/mL). Distribution of the cell cycle was determined by flow cytometry (FACSCalibur; Becton Dickinson) as described[17].

Apoptosis and necrosis

Cells (10^5 cells per well) were grown in six-well plates in growth medium overnight and medium was replaced by fresh growth medium, adding aphidicolin for another 24 h at three concentrations that showed either no, modest, or maximal effect on [^{3}H]thymidine incorporation. Then cells were trypsinized and washed with binding buffer (10 mM HEPES/NaOH pH 7.4, 140 mM NaCl, 2.5 mM $CaCl_2$). Apoptosis was determined by flow cytometric detection (FACSCalibur, Becton Dickinson) of phosphatidylserine translocation using annexin V-FITC (Axxora, Grünberg, Germany; 0.5 µg/mL)[20]. Discrimination between early apoptotic cells (annexin V^+/PI^-) and late apoptotic and necrotic cells (annexin V^+/PI^+) was achieved by simultaneous measurement of exclusion of the non-vital dye PI (1 µg/mL) as described[21].

RNA extraction and semiquantitative PCR

mRNA of normal human keratinocytes, HaCaT cells, and SCC-25 cells was isolated using the QuickPrep Micro mRNA Purification Kit (Amersham) according to the manufacturer's instructions. Aliquots of the mRNA preparation were kept frozen at –80°C until used. One microgram of mRNA was reverse transcribed in the presence of 1 pmol of a 25–30mer oligo(dT) primer. Two primers representing specific oligonucleotides were designed based on the nucleotide sequences of the respective enzyme or transporter (Table 1). PCR amplification was carried out in a thermocycler (T Gradient; Whatman Biometra, Göttingen, Germany) using GenTherm DNA polymerase under the following cycling conditions: (1) 94°C for 1 min; (2) 94°C for 1 min; (3) 55°C for 1 min; (4) 72°C for 1 min; (5) repetition of steps 2–4 for 29 cycles; (6) 72°C for 2 min; and (7) 4°C for 1 min. Polymerase chain reaction products were size-fractionated in agarose gel (2%), and visualized by ethidium bromide staining.

Statistics

GraphPad Prism Software Version 4.02 (GraphPad Software, San Diego, CA, USA) was used for curve fitting and calculation of –log IC_{50} values. Arithmetic mean ± standard error was calculated from three independent experiments which were each performed in triplicate. Mean –log IC_{50} served to calculate IC_{50} (µM) in addition, which is also reported in

Table 1. Primer sequences for RT-PCR[a].

Gene	Forward primer	Reverse primer	length
MRP4	CCA TTG AAG ATC TTC CTGG	GGT GTT CAA TCT GTG TGC	239 bp
MRP5	AGC TGG GTA CTT CCA GAG CA	TCT GTC AAC AGC CAC TGA GG	217 bp
hENT-1 Iso1	AGT GGC TCG GAG CTA TCA GA	GGG CTG AGA GTT GGA GAC TG	237 bp
TK-1	CTT GAG GAG TAC TCG GGT TCG TG	CTT TTT CCT GAG AAC ATC GGC	115 bp
TPace	CTG CTG TAT CGT GGG TCA GA	CCT CCG AAC TTAACG TCC AC	171 bp
dCK	AGC AAG GCA TTC CTC TTG AA	AAC CAT TTG GCT GCC TGT AG	226 bp
dGK Iso1	GCT GGT GTT GGA TGT CAA TG	AGA GTG CTC CAG GGA TGA GA	210 bp
GAPDH	ATG CAA CGG ATT TGG TCG TAT	TCT CGC TCC TGG AAG ATG GTG	221 bp

Note. Iso1, isoform 1.

[a]cDNA sequences were obtained from the National Institutes of Health Gene Bank. The table shows the sequences and the expected PCR product size (length) of MRP 4, MRP 5, hENT-1, TK-1, TPace, dCK, dGK, and GAPDH.

the text. Cell death data of drug treated samples were compared to those of the respective control by Student's *t*-test; $p \leq 0.05$ was considered to indicate a difference. Samples from the MTT test, NRU, and thymidine incorporation assay were compared to controls by one-way analysis of variance (ANOVA) followed by Dunnett's test, using the built-in statistical analysis package of GraphPad Prism Software; $p \leq 0.05$ was considered to indicate a difference. Regarding thymidine incorporation (SCC-25) following doxorubicin stimulation, one outlier (10^{-7} M) was eliminated.

Cells exposed to the respective solvent served as control. Reduction was calculated after non-linear regression as 100 – *E*, where *E* is the activity at 10^{-4} M in percent; n.d. indicates not determinable.

Results

Our 3D model of DNA pol α enabled us to identify three promising inhibitors of the enzyme. The agents were synthesized and subjected to pharmacological testing in comparison to aphidicolin, 5-FU, and diclofenac.

Molecular modeling: development, docking, and molecular dynamics simulations of HM-1-TP, BuP-OH-TP, and iso-Hex-OH-TP

Docking of the natural substrate of pol α desoxythymidine-triphosphate (dTTP) into the active site model revealed the formation of a hydrogen bond between the amide hydrogen of Tyr865 and the oxygen of the 3'-OH group of the ribose[12]. Consequently, a carbonyl function instead of the hydroxyl group in position 3' could lead to an even better H-bond acceptor. Docking studies with this compound (HM-1-TP) confirmed our suggestion, as illustrated in Figure 1. The length of the detected hydrogen bond between the carbonyl oxygen and Tyr865 amounted to 2.25 Å.

Recently, we studied and described the binding mode of the known nucleotide analog pol α inhibitor 2-butylanilino-dATP (BuP) with molecular modeling methods[12]. Molecular dynamics simulations of BuP suggested the possibility of an additional H-bond formation with Tyr865. Thus, the introduction of a hydroxyl group in the *ortho*-position to the butyl moiety of the butylanilino group of BuP led us to the new ligand BuP-OH-TP. Indeed, molecular dynamics simulations showed the existence of a stable H-bond of the OH group with Tyr865 (Figure 2). A series of BuP-OH analogs have been studied in detail with respect to their potential interaction geometries as well as affinities to the pol α active site. The results will be reported elsewhere[22].

Chemistry

The strategy toward the synthesis of ketothymidine **1** required the use of a labile protecting group for the primary hydroxyl group of the nucleoside. It is known that 2'-deoxyribonucleosides bearing a keto group in position 3' are fairly unstable and tend to easily eliminate the nucleobase in the presence of a base or silica gel[23,24]. Efficient preparation of the 3'-ketothymidine **1** therefore depends to a large extent on rapid isolation of the product, which led us to choose dimethoxytrityl protection. For synthesis of the target compound **1** (Scheme 2) we started from thymidine, which was regioselectively protected as dimethoxytrityl ether at the primary alcohol position[16]. The remaining secondary alcohol group of intermediate **14** was smoothly oxidized employing the Dess–Martin reagent[25] to quantitatively provide furanone derivative **15**. Deprotection with trifluoroacetic acid furnished **1** in 69% yield (purity ca. 95% according to NMR spectrum). Further purification by crystallization or flash chromatography was not possible, because of the fast decomposition of the product in various solvents and on silica gel or alumina.

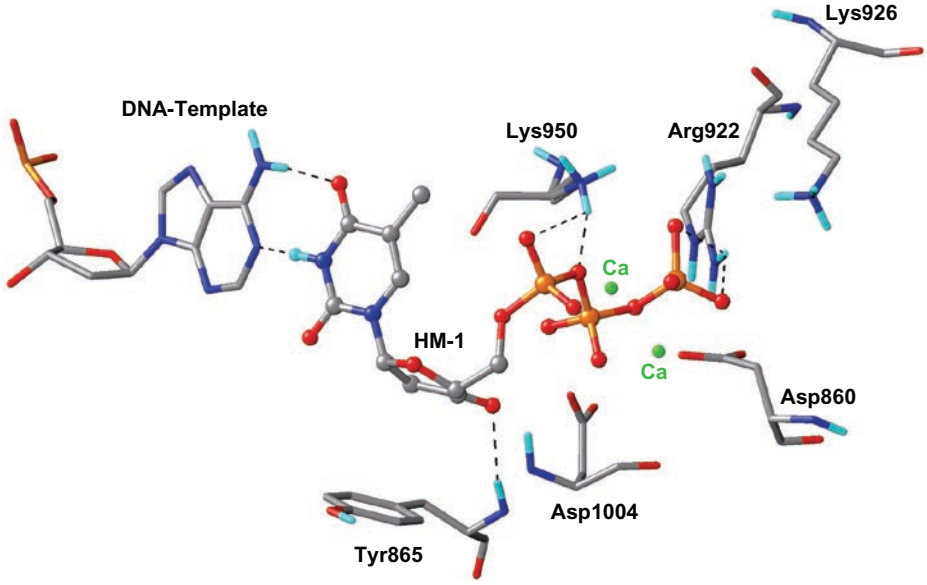

Figure 1. Docking of HM-1-TP into the active site model of pol α: H-bond formation of the carbonyl function of HM-1-TP with the amide hydrogen of Tyr865.

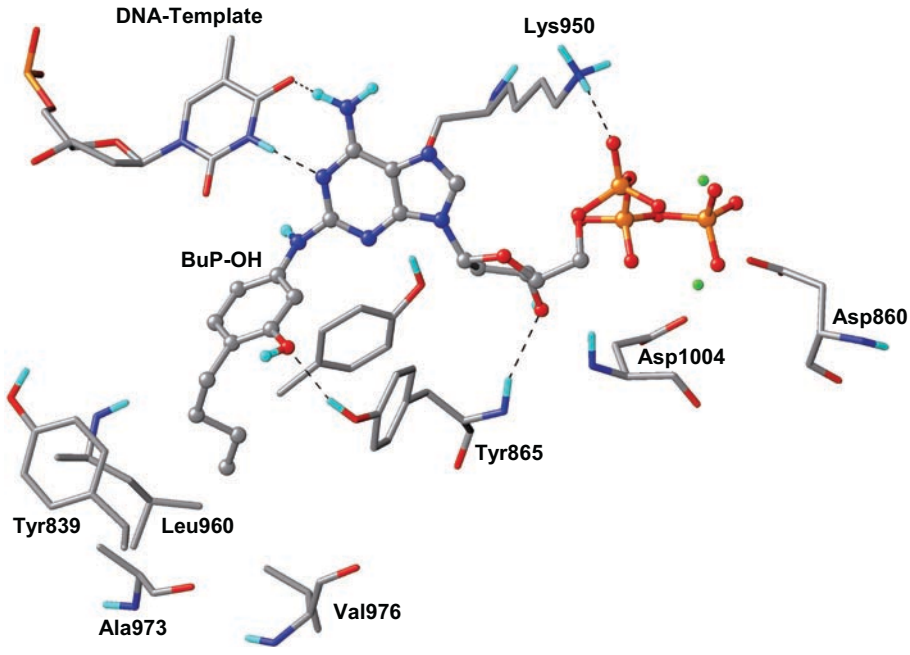

Figure 2. Docking of BuP-OH-TP into the active site model of pol α: H-bond formation of the hydroxyl group in *ortho*-position to the butyl moiety of BuP-OH-TP with Tyr865.

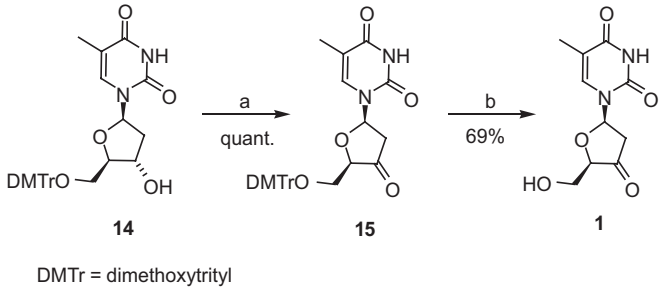

Scheme 2. Synthesis of compound **1** (HM-1). Reagents and conditions: (a) Dess–Martin reagent, CH_2Cl_2, 0°C, then room temperature; (b) TFA, CH_2Cl_2, 0°C.

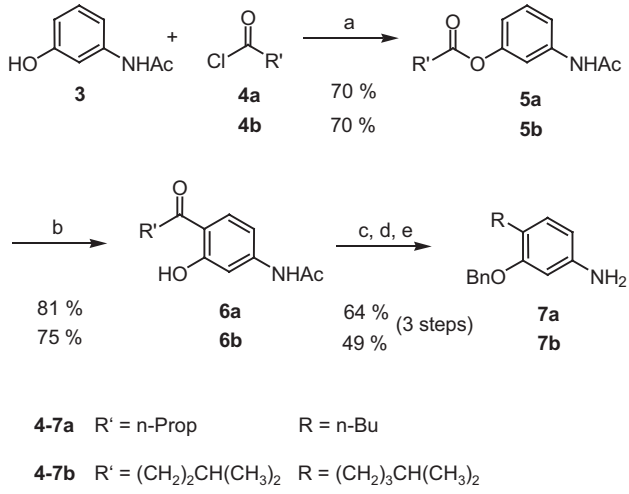

Scheme 3. Synthesis of compounds **7a** and **7b**. Reagents and conditions: (a) pyridine, toluene, 95°C; (b) $AlCl_3$, 130°C; (c) H_2, Pd on charcoal, $MeSO_3H$, AcOH, EtOAc, EtOH; (d) BnBr, K_2CO_3, acetone, 70°C; (e) KOH, MeOH, H_2O.

For the synthesis of compounds **2a** and **2b** (Scheme 5), three phases could be defined which, in part, follow the established route leading to nucleotide analog 2-butylanilinoadenine[26]. First, aniline derivatives **7a** and **7b** were prepared via straightforward sequences (Scheme 3). After acylation of 3-acetamidophenol **3** with the appropriate acid chlorides **4a** and **4b,** the resulting aryl esters **5a** and **5b** were subjected to a Lewis acid promoted Fries rearrangement. For this purpose, aluminum chloride was employed as already published for the preparation of compound **6a**[14]. The rearrangements smoothly furnished the *para*-acylated aniline derivatives **6a** and **6b**. After reduction of the carbonyl group with hydrogen under palladium catalysis, *O*-benzylation, and amide hydrolysis, the required aniline derivatives **7a** and **7b** were obtained in satisfactory overall yields.

In the second phase for the preparation of target compounds **2a** and **2b** (Scheme 5), we connected the substituted aniline derivatives **7** with the purine moiety (Scheme 4). This was achieved by a regioselective nucleophilic substitution employing 2-bromohypoxanthine **8** and compounds **7a** and **7b**[26]. The required 2-arylated guanine derivatives **9a** and **9b** were obtained in 90% and 81% yield, respectively. Treatment of these intermediates with phosphorus oxychloride in the presence of *N*,*N*-dimethylaniline at 110°C converted the purine carbonyl group of **9a** and **9b** into a chloro substituent in the required 6-position, affording chloropurine derivatives **10a** and **10b** in excellent yields.

The final phase of the sequence (Scheme 5) first involved glycosidation of the 6-chloropurines **10a** and **10b** employing 2-deoxy-3,5-di-*p*-toluyl-D-ribofuranosyl chloride **11** as suitably protected carbohydrate donor[15]. The resulting products **12a** and **12b** were isolated in ~50% yield. Only one diastereomer was isolated in each of these reactions; however,

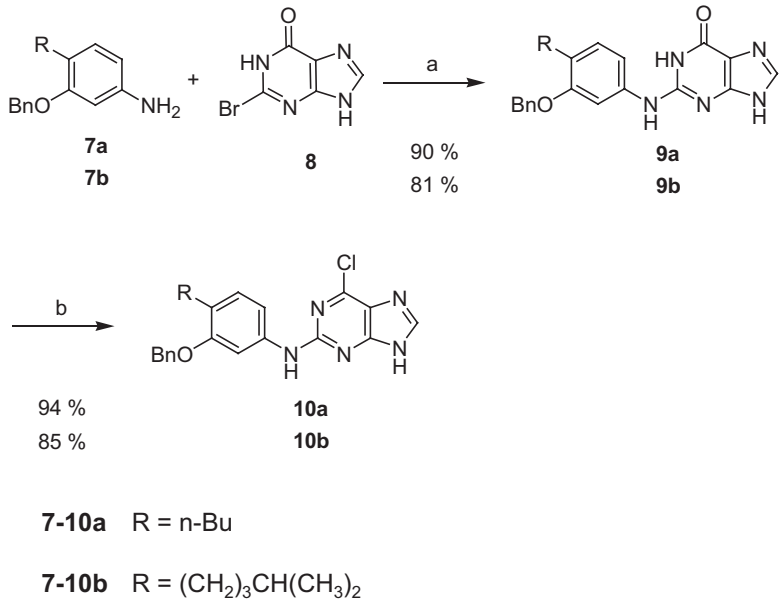

Scheme 4. Synthesis of compounds **10a** and **10b**. Reagents and conditions: (a) $CH_3OCH_2CH_2OH$, H_2O, 120°C; (b) $POCl_3$, *N*,*N*-dimethylaniline, 110°C.

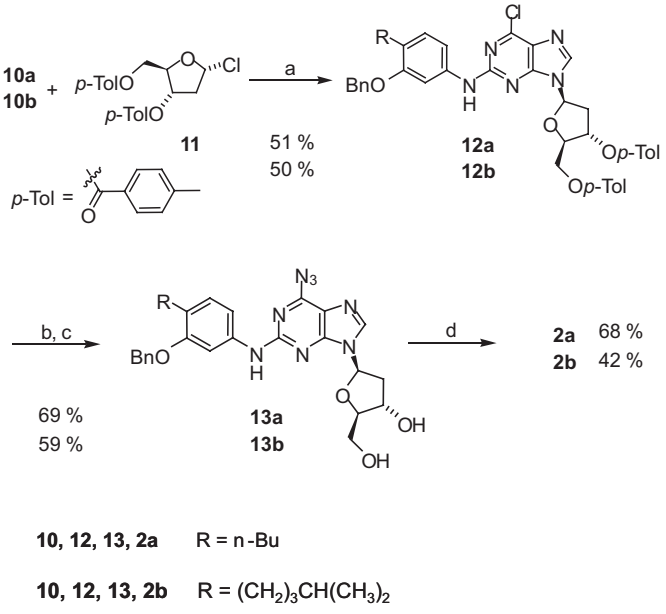

Scheme 5. Synthesis of compounds **2a** (BuP-OH) and **2b** (iso-Hex-OH). Reagents and conditions: (a) NaH, acetonitrile; (b) NaN_3, DMF, 60°C; (c) NaOMe (0.5 N in MeOH); (d) H_2, Pd-black (5%), HCO_2H in MeOH.

in the case of **12a**, ~10% of the unwanted 7-β-isomer was formed. For the crucial introduction of nitrogen in position 6 of the purine core, we transformed the 6-chloro compounds **12a** and **12b** into 6-azido derivatives **13a** and **13b** in 69% and 59% yield, respectively. These intermediates exist as mixtures of tautomers with the azido form as depicted in Scheme 4 and their corresponding tetrazol form (for a brief comment on azido-tetrazolo tautomery of the 2-amino-6--azido purine system see references 27 and 28). The NMR spectra were not suitable to exactly determine the ratio of isomers. Unfortunately, the conversion of these intermediates to give target compounds **2a** and **2b** turned out to be rather difficult. Fairly large amounts of palladium-black had to be employed to convert the azido group into the amino function and to perform the final deprotection of **13a** and **13b**. The *O*-debenzylation was the slow step, and in several experiments we obtained mixtures with compounds still bearing the benzyloxy group. However, sufficient amounts of palladium-black and long reaction times finally provided target compounds **2a** and **2b** in good or moderate yield and with reasonable purity.

Biological properties: cytotoxic potency of reference compounds, expression of potential enzymes, and transporters of nucleotide metabolism

In contrast to molecular modeling, for which the triphosphates of the nucleoside analogs were necessary, cellular toxicity was investigated with the nucleoside analogs themselves. The triphosphates of the substances would be too hydrophilic to permeate the cell membrane and even more the horny layer when applied topically. The phosphorylation of the substances is done intracellularly by specific cellular kinases. To investigate whether pol α inhibition may be an option for actinic keratosis and cutaneous squamous cell carcinoma therapy, we first compared the effects of aphidicolin to those of drugs approved for actinic keratosis (5-FU, diclofenac/hyaluronic acid) and the highly cytotoxic doxorubicin. The pyrophosphate analog foscarnet, blocking the pyrophosphate binding site of viral pol α, served as negative control, which in fact proved inactive (at maximum 20% reduction of proliferation with NHK and SCC-25 cells, 9% reduction of viability with SCC-25 cells and none with normal keratinocytes). Besides NHK and SCC-25 cells, HaCaT cells were also tested. These, however, turned out to be more susceptible to the drugs of interest than the slower-dividing normal keratinocytes and tumor cells. Therefore, results had to be interpreted with caution, and are reported only if considered relevant.

Inhibition of DNA synthesis

As derived from thymidine incorporation, aphidicolin 10^{-6} M completely inhibited DNA synthesis in NHK cells, and the IC_{50} value was in the submicromolar range (–log IC_{50} 7.08 ± 0.05, active concentration ~0.083 μM). Yet SCC-25 cells were less sensitive, with an IC_{50} value in the micromolar range and a maximum inhibition of 57% (Table 2). Diclofenac 10^{-5} M induced a moderate effect (~20% inhibition) in NHK cells, while no proliferation was seen at 10^{-4} M (–log IC_{50} 4.16 ± 0.22, active concentration ~69 μM). In SCC-25 cells DNA synthesis was also significantly inhibited (–log IC_{50} 4.28 ± 0.27, active concentration ~52 μM), but once more maximum inhibition (47% at 10^{-4} M) was less than in normal keratinocytes (complete inhibition). In mice, diclofenac failed to interfere with keratinocyte proliferation in a surgical wound model[29] while suppressing fibrosarcoma tumor growth[30]. Doxorubicin did not differentiate between NHK and SCC-25 cells. It caused 100% inhibition and –log IC_{50} values were ~7 (active concentrations ~0.04–0.10 μM) with NHK and SCC-25 cells, respectively.

Viability

Cell viability was determined by measuring formazan formation by the mitochondrial reductase system (MTT reduction test). Only viable and metabolically active cells will produce the dye, and thus the amount of dye is set in direct proportion to the cell number. This method allowed verification of the data derived from the proliferation assay, as well as the study of 5-FU cytotoxicity. 5-FU was clearly less potent as compared to aphidicolin. This held true with respect to both –log IC_{50} and maximum inhibition of viability. A relevant difference between normal and transformed keratinocytes was not detected (Table 2).

Membrane effects

Despite the nuclear target, membrane integrity was tested, too, using the NRU assay. The uncharged, vital dye readily penetrates cell membranes by non-ionic diffusion and accumulates within the acidic lysosomes, and is excluded by membrane destruction resulting in reduced dye accumulation or increased release of the dye. The maximum effect of aphidicolin on NRU was negligible with keratinocytes (8% decline of dye accumulation), but marked with SCC-25 cells (61%, Table 2). The maximum effect of 5-FU on NRU in normal keratinocytes was also less than in the MTT test, yet more pronounced (23%) than following aphidicolin stimulation. In SCC-25 cells, 5-FU also reached a value of 64% reduction. The active concentrations (–log IC_{50}) of both aphidicolin and 5-FU were rather close when studying NRU and viability (Table 2).

Aphidicolin induced cell death

In order to verify that aphidicolin does not only inhibit proliferation but actually provokes cell death, flow cytometry was used to quantify the number of cells undergoing apoptosis. Sensitivity of keratinocytes and HaCaT cells appeared similar, if the cells were exposed to aphidicolin. As anticipated, the SCC-25 cell line was least sensitive (Figure 3).

Expression of enzymes of nucleotide metabolism and nucleotide transporters

Next we studied the expression of enzymes and outward transporters for relevant nucleosides and nucleotides, respectively. On the mRNA level we were able to detect the cytosolic enzymes deoxycytidine kinase (dCK), thymidine kinase-1, and thymidine phosphorylase, as well as the mitochondrial enzyme deoxyguanosine kinase (dGK) (Figure 4A). We also detected the nucleoside transporter hENT-1 and the anionic outward transporters MRP 4 and MRP 5 (Figure 4B). SCC-25 cells hardly expressed hENT-1 and dCK. For all other enzymes and transporters no relevant differences between normal keratinocytes, HaCaT cells, and SCC-25 were seen.

Cytotoxicity of nucleosides proposed by molecular modeling

According to previous results, nucleoside analogs may have the potential to interfere with the proliferation and viability of SCC-25 cells. A tumor-selective effect should be most welcome, since this is widely lacking with current drugs, in particular 5-FU, whereas the standard pol α inhibitor,

Table 2. Activity of polymerase α inhibitors.

	–log IC_{50} [M] ± SE (reduction (10^{-4} M)			
	Aphidicolin	5-FU	HM-1	BuP-OH
Viability (48 h)				
NHK	8.24 ± 0.40 (45%)	5.25 ± 0.52 (36%)	n.d. (23%)	4.21 ± 0.30 (62%)
SCC-25	6.28 ± 0.29 (62%)	5.97 ± 0.27 (45%)	4.35 ± 0.43 (47%)	4.69 ± 0.26 (72%)
Membrane damage (48 h)				
NHK	n.d. (8%)	n.d. (23%)	n.d. (14%)	4.43 ± 0.15 (57%)
SCC-25	5.99 ± 0.32 (61%)	5.66 ± 0.21 (64%)	5.16 ± 0.36 (31%)	4.65 ± 0.22 (62%)
Inhibition of DNA synthesis (72 h)				
NHK	7.08 ± 0.05 (100%)	Assay of [^{3}H]thymidine incorporation not possible with thymidine analogs		5.96 ± 0.15 (99%)
SCC-25	6.17 ± 0.38 (57%)			4.62 ± 0.41 (81%)

Note. –log IC_{50} values [M] + standard error derived from reduction in viability (MTT test), membrane damage (neutral red uptake; NRU assay), and thymidine incorporation. Normal human keratinocytes (NHK) and SCC-25 cells were incubated with the indicated agents (10^{-10} M to 10^{-4} M). Cells exposed to the respective solvent served as control. Three independent experiments were performed in triplicate. After non-linear regression giving the dose–response curves, reduction of viability and thymidine incorporation was calculated as 100 – *E*; *E* is activity at 10^{-4} M in percent, and the calculated point of inflection gave the –log IC_{50} value; n.d., –log IC_{50} not determinable with maximum inhibition <30%.

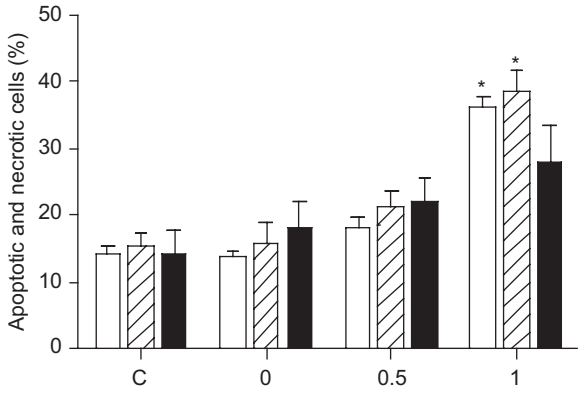

Figure 3. Apoptotic and necrotic cells (% of total cell population) following aphidicolin exposure. Normal keratinocytes (open bars), SCC-25 cells (closed bars), and HaCaT cells (hatched bars) were incubated for 24 h at concentrations provoking either no inhibition of proliferation (0) or half maximal (0.5) or maximal (1) inhibition. Then the cells were subjected to flow cytometry. Early apoptosis was determined by phosphatidylserine translocation using annexin V-FITC labeling and simultaneous exclusion of propidium iodide (annexin V^+/PI^-). Late apoptotic and necrotic cells were annexin V^+/PI^+. DMSO served for control (C). Mean ± SE of three independent experiments are depicted; $*p \leq 0.05$.

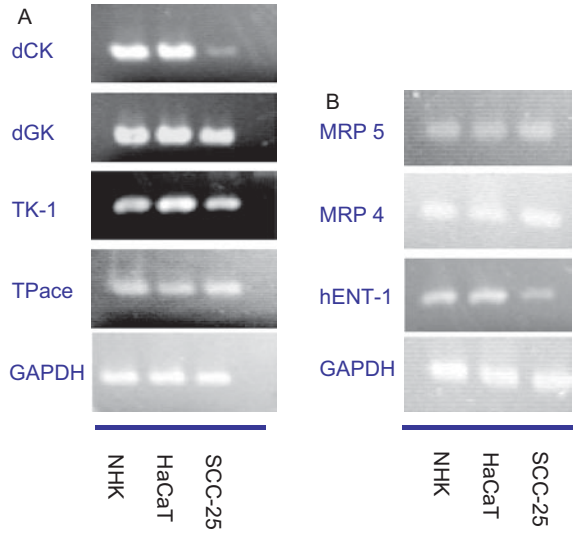

Figure 4. Expression of enzymes of nucleotide metabolism (A) and relevant transporters (B) in normal (NHK) and transformed (HaCaT, SCC-25) keratinocytes. Except for the deoxycytidine kinase (dCK, A) and the human equilibrative nucleoside transporter (hENT-1, B) hardly expressed in SCC-25 cells, the expression of thymidine kinase-1 (TK-1), thymidine phosphorylase (TPace), and deoxyguanosine kinase (dGK) as well as the anionic outward transporters MRP 4 and MRP 5 did not differ between normal and transformed keratinocytes at the mRNA level. Isolated mRNA was reverse transcribed using specific oligonucleotide primers (for primer sequences refer to Table 1), amplified (30 cycles), and visualized by ethidium bromide staining; GAPDH expression served for reference. The experiment was repeated twice with comparable results.

aphidicolin, preferentially damages normal keratinocytes. Cytotoxicity of the modeled nucleosides was compared to the aphidicolin and 5-FU effects. Table 2 shows –log IC_{50} values and maximum reduction of proliferation (thymidine incorporation) and viability (MTT test) as well as membrane damage (neutral red uptake) in NHK and SCC-25 cells.

Viability

All proposed nucleosides appeared active, yet missed the potency of aphidicolin either with respect to both –log IC_{50} and maximum inhibition of viability (HM-1, iso-Hex-OH) or at least with respect to –log IC_{50} (BuP-OH). In fact, the maximum inhibitory capacity of aphidicolin was even superseded by BuP-OH regarding NHK and SCC-25 cells. Differences in the modeled nucleosides with respect to 5-FU, however, were less obvious, and maximum effects were even more pronounced with BuP-OH and iso-Hex-OH. Nevertheless, iso-Hex-OH failed to meet our expectations based on the results of ligand docking, while the IC_{50} values (NHK 38.9 μM; SCC-25 31.6 μM) were close to those of BuP-OH (NHK 60.7 μM; SCC-25 20.4 μM; Table 2); maximum cytotoxicity in SCC-25 cells amounted to only 54% (NHK 46%). Most interestingly, a distinct selectivity for SCC-25 cells was observed when studying HM-1 (Table 2). Further testing was focused on BuP-OH and HM-1, eliminating iso-Hex-OH from the study panel.

Inhibition of DNA synthesis

After 48 h BuP-OH strongly inhibited the proliferation of normal keratinocytes. The maximum inhibition of SCC-25 cell proliferation by BuP-OH even surmounted inhibition by aphidicolin (81% vs. 57%, Table 2). In fact, toxic concentrations of BuP-OH were close in NHK cells and SCC-25 cells (IC_{50} values: NHK 1.096 μM; SCC-25 23.99 μM); the purine derivative, however, was less potent than aphidicolin (IC_{50} values: NHK 0.083 μM; SCC-25 0.676 μM). The inhibitory effect of HM-1 on proliferation was not tested with the thymidine uptake assay since exogenous thymidine probably antagonizes the thymidine analog HM-1 — as well as the 5-FU related depletion of endogenous dTTP — and thus may antagonize an antiproliferative effect[31].

Membrane effects

BuP-OH did not differentiate between the cell types, and the active concentrations were about 10-fold higher as compared to aphidicolin and 5-FU. Once more, HM-1 appeared least active yet able to discriminate between transformed and normal keratinocytes (Table 2).

Time dependency

We also studied the time dependency of maximum cytotoxic effects. Results of the MTT test are depicted in Figure 5, comparing NHK and SCC-25 cells. Stimulation with aphidicolin showed no time dependency in any cell type tested or cytotoxicity test used. 5-FU and BuP-OH appeared more effective after 48 h than after 24 h in both cell types; once more, SCC-25 cells seemed to be more sensitive to treatment than NHK, probably due to increased metabolic activity. In contrast, HM-1 appeared more toxic at 24 h; obviously keratinocytes — both normal and transformed — can overcome thymidine depletion to some extent over time. Interestingly, BuP-OH inhibits cell proliferation of SCC-25 cells more efficiently after 24 h whereas in primary keratinocytes the differences are not marked

(data not shown). However, no relevant differences could be detected in the NRU assay after 24 h or 48 h stimulation time (data not shown).

Cell cycle distribution

Aphidicolin and 5-FU influenced cell cycle distribution in an expected manner. At 10^{-6} M both substances increased the fraction of cells in the S-phase, while higher aphidicolin concentrations induced cell death in SCC-25 cells. In normal keratinocytes an increase in G1 cells was shown. Most probably, this fraction also contains dead cells, as demonstrated by flow cytometry (Figure 6). Since primary keratinocytes do not undergo DNA laddering during apoptosis[32], they do not show a sub-G1 fraction in cell cycle analysis. Most interestingly, at 10^{-4} M HM-1 appeared more active than BuP-OH, causing an increase in the G2 phase in primary keratinocytes and a sharp increase in the sub-G1 peak in SCC-25 cells. This cytotoxic effect on non-contact-inhibited SCC-25 cells could be verified by the MTT test. Exposing SCC-25 cells to HM-1 10^{-4} M for 48 h, the viability declined by 77% when grown without contact-inhibition and by 43% when contact-inhibited seeding was used (10^4 and 4×10^4 cells per well), respectively.

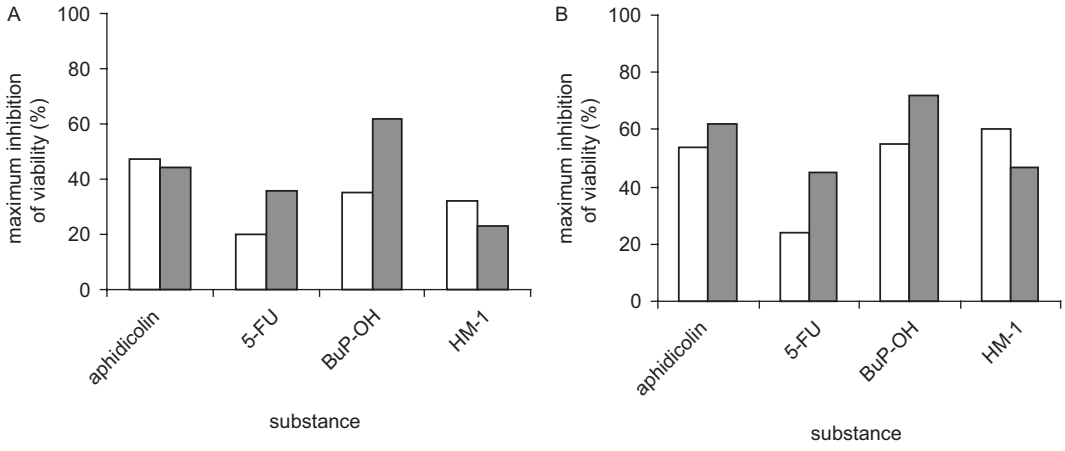

Figure 5. Time dependency of cytotoxicity (MTT test) in normal human keratinocytes (A) and SCC-25 cells (B) after stimulation with the agents of interest 10^{-4} M for 24 h (open bars) and 48 h (shaded bars), respectively. In contrast to aphidicolin and HM-1, 5-FU and BuP-OH appeared more active when applied for 48 h. Mean values of three independent experiments.

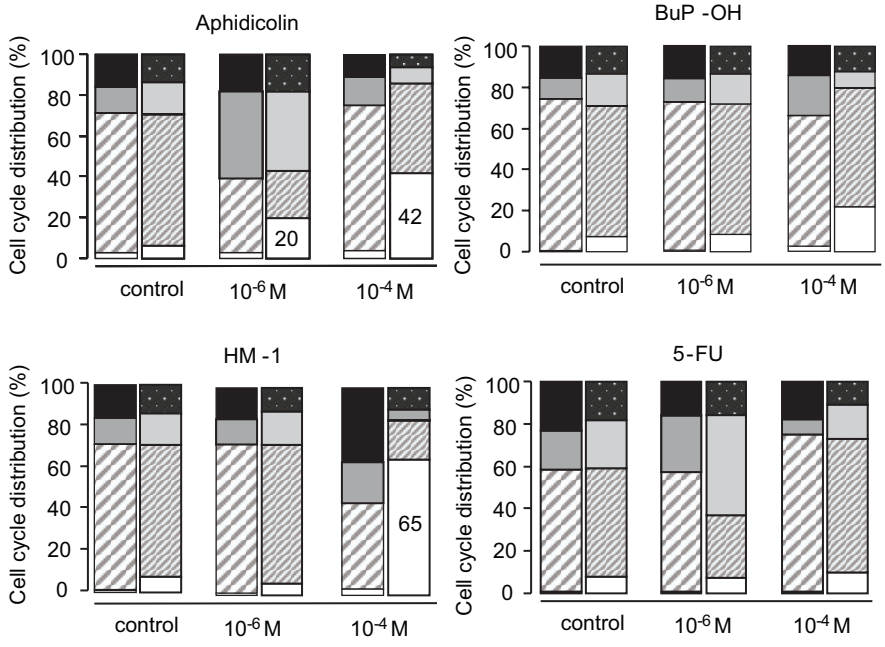

Figure 6. Cell cycle distribution of normal human keratinocytes (left bars) and SCC-25 cells (right bars). Keratinocytes grown without contact inhibition were stimulated with the test agents at two concentrations for 48 h. Aphidicolin and 5-FU increased the fraction of cells in the S-phase; aphidicolin (10^{-6}, 10^{-4} M) and HM-1 (10^{-4} M) appeared cytotoxic in SCC-25 cells. Cell cycle phases: sub-G1 (open part), G1 (hatched), S (shaded), G2 (closed). Mean values of three independent experiments.

Discussion

Nucleoside and non-nucleoside pol α inhibitors are not only relevant for research in the field of molecular biology but are also used for the treatment of leukemia, some solid tumors, and — most importantly — viral infections. Thus, these agents may offer a new approach also for skin cancer, if active by the topical application route used to control unwanted side effects. In fact, aphidicolin has not been introduced into therapy because of toxicity and rapid metabolism after systemic application[33].

We started our experimental studies by testing aphidicolin, the standard agent for the inhibition of pol α, which interferes with nucleotide incorporation into the elongated DNA during the S phase. Well in accordance with molecular modeling results[12], aphidicolin inhibited cell proliferation (Table 2; IC_{50}: SCC-25 0.676 μM; NHK 0.083 μM) by inhibition of DNA synthesis (Figure 6), but also by induction of apoptosis and necrosis (Figure 3) in transformed and normal human keratinocytes. As a consequence, cell viability declined and vital dye accumulation failed (IC_{50}: SCC-25 0.525 μM; NHK 0.0058 μM). Importantly, the various assays following stimulation with aphidicolin showed no selectivity for the tumor cell line (Table 2). In fact, DNA synthesis as well as mitochondrial function of normal keratinocytes appeared most sensitive. With respect to both maximum inhibition and IC_{50} values, viability and proliferation of normal keratinocytes were even influenced more strongly than viability and proliferation of SCC-25 cells (Table 2), which clearly demonstrates the non-suitability of aphidicolin in skin tumor therapy. Results from the NRU assay are well in accordance, although the effect on cell viability was always more pronounced.

Further reference substances were two drugs used in the therapy of actinic keratosis, i.e. 5-FU and diclofenac, as well as another cytotoxic drug, doxorubicin. As to be expected, pronounced toxic effects were also seen with doxorubicin, yet the agent does not differentiate between normal and transformed keratinocytes, –log IC_{50} values of the inhibition of proliferation being ~7 (IC_{50}: SCC-25 0.103 μM; NHK 0.042 μM). 5-FU differentiated between NHK (cytotoxicity IC_{50} 5.62 μM) and SCC-25 cells (IC_{50} 1.07 μM) to a limited extent. Diclofenac inhibits cyclooxygenase-2 (COX-2) activity, although the latter mechanism is not generally accepted[34]. In fact, we observed diclofenac-induced inhibition of keratinocyte proliferation (IC_{50}: NHK 69.2 μM; SCC-25 52.5 μM) whereas cyctoxicity was not seen. Thus, proliferation inhibition may add to the improvement of actinic keratosis.

We began our experiments with three types of keratinocytes, i.e. normal cells, HaCaT cells, and SCC-25 cells. However, as seen in cell cycle analysis, the rapidly dividing cell line HaCaT showed a greater percentage of cells in the S-phase, and therefore was more sensitive to aphidicolin and 5-FU (data not shown). Hence, HaCaT cells cannot be recognized as a model for normal keratinocytes, and we excluded them from cytotoxicity testing.

Applying molecular modeling methods, we were able to identify structurally new substances, which we assumed to be DNA pol α inhibitors. Though suggested by ligand docking to the active site of the enzyme, final proof of the proposed mechanism requires experiments exposing the activated nucleoside analog triphosphates to the isolated enzyme. We obtained the thymidine analog HM-1 **1** which was easily synthesized within a few steps. We could also prepare the desired target compounds BuP-OH **2a** and iso-Hex-OH **2b** in 11 steps, with low overall yields. Optimizations of the multistep approach to the purine derivatives for their synthesis on a larger scale — in particular for the very last steps — appear conceivable. Activity of these substances has been proved experimentally. The MTT reduction assay appeared very discriminative; regarding both IC_{50} values and maximum inhibition cytotoxicity, it ranked as follows: aphidicolin > BuP-OH > iso-Hex-OH, 5-FU, > HM-1 >> foscarnet (negative control). Correspondingly, thymidine incorporation ranked aphidicolin >> BuP-OH >> foscarnet and neutral red release aphidicolin, BuP-OH, 5-FU > HM-1. With BuP-OH (and 5-FU), cell viability was even more reduced after 48 h as compared to 24 h (Figure 5). However, with aphidicolin no such difference could be seen. Taking IC_{50} values and maximum inhibitory effects into consideration, we were thus able to predict structures of DNA pol α inhibitors, and the range order of activity in general met our expectations. The model was predictive, given that the ligands had unhindered access to the active site of the enzyme. This was obviously not true with non-linear substituents at the side chain (compound **2b**, iso-Hex-OH). According to the modeling data, iso-Hex-OH (SCC-25: IC_{50} 38.9 μM and 54% maximum inhibition) should be more active as compared to BuP-OH (SCC-25: IC_{50} 20.4 μM and 72% maximum inhibition), yet this was not seen in the MTT test and iso-Hex-OH was excluded from further experiments.

The tumor cell specifity of HM-1, which may be linked to differences in nucleotide metabolism and transporters (Figure 4), was not conceivable by molecular modeling. Moreover, HM-1 turned out to be most active in cell cycle analysis (Figure 6), and the unexpected high cytotoxicity on SCC-25 cells (77% maximum inhibition) even surmounted aphidicolin effects in non-contact-inhibited cells. We also found a time dependency of the effects on viability of the nucleoside analog HM-1, which was more toxic after 24 h incubation time compared to 48 h incubation, whereas 5-FU and BuP-OH were more effective after 48 h treatment (Figure 5). No differences between 24 h or 48 h stimulation were detected in the NRU assay. It is not known whether keratinocytes or SCC-25 cells possess a mechanism to overcome the cytotoxicity of HM-1 with prolonged incubation.

DNA pol α can be considered as a relevant target for the treatment of actinic keratosis and squamous cell carcinoma, if given nucleoside inhibitors are activated in the tumor cell and fit into the catalytic domain of very restricted size[12]. While the latter appears possible by docking drug candidates into the modeled binding site of pol α, the activation of nucleoside and nucleotide derivatives within the cells and the ability to actually inhibit pol α is not to be predicted

currently. Since aphidicolin does not depend on intracellular activation, the current experiments do not allow any conclusion in this respect. However, we were able to detect important nucleoside kinases in all types of keratinocytes tested (Figure 4A). TK-1, responsible for activation of thymidine and analogs, as well as the mitochondrial enzyme dGK, activating deoxyguanosine and analogs, were on the one hand detected in all cell types. On the other hand, the cytosolic enzyme dCK, with the broadest substrate spectrum, was hardly detected in SCC-25 cells but was detected in normal and transformed keratinocytes. We therefore suppose that the activation of HM-1 is readily possible and explains its cytotoxicity (Table 2). However, the activation route of BuP-OH has yet to be confirmed. Besides a cytosolic activation through dCK, a mitochondrial activation through dGK might be possible as it was also shown for nelarabine (Ara-G)[35]. Thymidine phosphorylase could be also detected in all cell types. This enzyme on the one hand allows 5-FU activation also via the so-called DNA route, but on the other hand it may cause resistance.

The expression of inward and outward transporters was also investigated in skin cells (Figure 4B). MRP 4 and MRP 5, anionic outward transporters, which may cause resistance if they are overexpressed, could be detected in normal and transformed keratinocytes, but not in a great amount. The expression of MRP 4 and MRP 5[36] as well as various organic anion transporters of the OATP family[37] in NHK cells has been described previously. Yet the ubiquitously occurring nucleoside transporter hENT-1 again could not be detected in SCC-25 cells, although it did occur in normal keratinocytes and HaCaT cells. Whether this may explain the tumor cell specifity of HM-1 (Table 2), however, currently remains unclear, since it is not yet proven via which route the nucleoside analogs are taken up by the cells. Yet, as thymidine and purine analogs proved effective also in SCC-25 cells, an alternative route via another transporter or independent of a transporter, e.g. via endocytosis, might also be possible. Importantly, nucleoside analogs identified by molecular modeling might overcome the lack of selectivity for tumor cells and the rapid recovery from aphidicolin treatment which is even followed by rebound thymidine incorporation at 48 h[13].

Conclusion

In conclusion, molecular modeling allowed us to identify nucleoside analogs which proved cytotoxic toward transformed but also toward normal human keratinocytes, and a further improvement of potency and selectivity may become possible by the development of analogs, e.g. of the phosphonate type which are of high potency, for example, in human immunodeficiency virus (HIV) infections.

Acknowledgements

The authors thank Novartis Pharma AG, Basel, Switzerland for supplying diclofenac and medac Gesellschaft für klinische Spezialpräparate mbH, Wedel, Germany for supplying doxorubicin.

Declaration of interest

Financial support of the German Ministry of Education and Research (13N9062 and 13N9061) is gratefully acknowledged. Two of the authors (H-D.H, M.S-K) are inventors of the respective patent applied for by RIEMSER Arzneimittel AG (Greifswald – Insel Riems), European Appl. No.: 07090098.0. Moreover, one of them (M.S.-K.) acts as a consultant for RIEMSER Arzneimittel AG (Greifswald – Insel Riems) with respect to the development of dermatics.

References

1. Jorizzo J. Topical treatment of actinic keratosis with fluorouracil: is irritation associated with efficacy? J Drugs Dermatol 2004; 3:21–6.
2. Rhodes LE, de Rie M, Enstrom Y, Groves R, Morken T, Goulden V, et al. Photodynamic therapy using topical methyl aminolevulinate vs surgery for nodular basal cell carcinoma: results of a multicenter randomized prospective trial. Arch Dermatol 2004;140:17–23.
3. Rivers JK, Arlette J, Shear N, Guenther L, Carey W, Poulin Y. Topical treatment of actinic keratoses with 3.0% diclofenac in 2.5% hyaluronan gel. Br J Dermatol 2002;146:94–100.
4. Lebwohl M, Dinehart S, Whiting D, Lee PK, Tawfik N, Jorizzo J, et al. Imiquimod 5% cream for the treatment of actinic keratosis: results from two phase III, randomized, double-blind, parallel group, vehicle-controlled trials. J Am Acad Dermatol 2004; 50:714–21.
5. Maeda N, Kokai Y, Ohtani S, Sahara H, Kuriyama I, Kamisuki S, et al. Anti-tumor effects of dehydroaltenusin, a specific inhibitor of mammalian DNA polymerase alpha. Biochem Biophys Res Commun 2007;352:390–6.
6. Kuriyama I, Musumi K, Yonezawa Y, Takemura M, Maeda N, Iijima H, et al. Inhibitory effects of glycolipids fraction from spinach on mammalian DNA polymerase activity and human cancer cell proliferation. J Nutr Biochem 2005;16:594–601.
7. Maeda N, Kokai Y, Ohtani S, Sahara H, Hada T, Ishimaru C, et al. Anti-tumor effects of the glycolipids fraction from spinach which inhibited DNA polymerase activity. Nutr Cancer 2007;57:216–23.
8. Matsubara K, Saito A, Tanaka A, Nakajima N, Akagi R, Mori M, Mizushina Y. Catechin conjugated with fatty acid inhibits DNA polymerase and angiogenesis. DNA Cell Biol 2006;25:95–103.
9. Matsubara K, Saito A, Tanaka A, Nakajima N, Akagi R, Mori M, et al. Epicatechin conjugated with fatty acid is a potent inhibitor of DNA polymerase and angiogenesis. Life Sci 2007;80:1578–5.
10. Gandhi V, Huang P, Chapman AJ, Chen F, Plunkett W. Incorporation of fludarabine and 1-beta-D-arabinofuranosylcytosine 5′-triphosphates by DNA polymerase alpha: affinity, interaction, and consequences. Clin Cancer Res 1997;3:1347–55.
11. Jiang HY, Hickey RJ, Abdel-Aziz W, Malkas LH. Effects of gemcitabine and araC on in vitro DNA synthesis mediated by the human breast cell DNA synthesome. Cancer Chemother Pharmacol 2000;45:320–8.
12. Richartz A, Höltje M, Brandt B, Schäfer-Korting M, Höltje HD. Targeting human DNA polymerase alpha for the inhibition of keratinocyte proliferation. Part 1.Homology model, active site architecture and ligand binding. J Enzyme Inhib Med Chem 2008;23:94–100.
13. O'Dwyer PJ, Moyer JD, Suffness M, Harrison SD Jr, Cysyk R, Hamilton TC, et al. Antitumor activity and biochemical effects of aphidicolin glycinate (NSC 303812) alone and in combination with cisplatin in vivo. Cancer Res 1994;54:724–9.
14. Julia M, Baillarge M.Keto derivs. of aminophenols by the Friedel-Crafts and the Fries reactions. Bull Chim Soc Fr 1952:639–42.
15. Hoffer M. Alpha-thymidine. Chem Ber 1960;93:2777–81.
16. Lan T, McLaughlin LW. Minor groove hydration is critical to the stability of DNA duplexes. J Am Chem Soc 2000;122:6512–13.
17. Vogler R, Sauer B, Kim DS, Schäfer-Korting M, Kleuser B. Sphingosine-1-phosphate and its potentially paradoxical effects on critical parameters of cutaneous wound healing. J Invest Dermatol 2003;120:693–700.

18. Gysler A, Lange K, Korting HC, Schafer-Korting M. Prednicarbate biotransformation in human foreskin keratinocytes and fibroblasts. Pharm Res 1997;14:793–7.
19. Liebsch M, Spielmann H. 3T3 NRU Phototoxicity Assay. Available at http://ecvam-dbalmjrcceceuint/public_view_doccfm?id=736F27E9E9F7A9D869FB48087878D2497180BB0BC12CB10496CDA74B54630A05A3291B895581F634, 1998.
20. Vermes I, Haanen C, Richel DJ, Schaafsma MR, Kalsbeek-Batenburg E, Reutelingsperger CP. Apoptosis and secondary necrosis of lymphocytes in culture. Acta Haematol 1997;98:8–13.
21. Manggau M, Kim DS, Ruwisch L, Vogler R, Korting HC, Schäfer-Korting M, et al. 1Alpha,25-dihydroxyvitamin D3 protects human keratinocytes from apoptosis by the formation of sphingosine-1-phosphate. J Invest Dermatol 2001;117:1241–9.
22. Zdrazil B, Höltje M, Schwanke A, Schmitz B, Schäfer-Korting M, Höltje H-D.Molecular modeling studies of new potential human DNA polymerase alpha inhibitors. 2009; submitted.
23. Hansske F, Madej D, Robins MJ. 2′ and 3′-Ketonucleosides and their arabino and xylo reduction products: convenient access via selective protection and oxidation of ribonucleosides. Tetrahedron 1984;40:125–35.
24. Sharma M, Bobek M. Synthesis of 2′,3′-dideoxy-3′-methylene pyrimine nucleosides as potential anti-AIDS agents. Tetrahedron Lett 1990;31:5839–42.
25. Samano V, Robins MJ. Nucleic acid related compounds. 60. Mild periodinane oxidation of protected nucleosides to give 2′-,and 3′-ketonucleosides. The first isolation of a purine 2′-deoxy-3′-ketonucleoside derivative. J Org Chem 1990;55:5186–8.
26. Wright GE, Dudycz LW, Kazimierczuk Z, Brown NC, Khan NN. Synthesis, cell growth inhibition, and antitumor screening of 2-(p-n-butylanilino)purines and their nucleoside analogues. J Med Chem 1987;30:109–16.
27. Frieden M, Avino A, Eritja R. Convenient synthesis of 8-amino-2′-deoxyadenosine. Nucleosides Nucleotides Nucleic Acids 2003;22:193–202.
28. Koshkin AA. Syntheses and base-pairing properties of locked nucleic acid nucleotides containing hypoxanthine, 2,6-diaminopurine, and 2-aminopurine nucleobases. J Org Chem 2004;69:3711–18.
29. Fedorocko P, Hoferova Z, Hofer M, Brezani P. Administration of liposomal muramyl tripeptide phosphatidylethanolamine (MTP-PE) and diclofenac in the combination attenuates their anti-tumor activities. Neoplasma 2003;50:176–84.
30. Hoferova Z, Fedorocko P, Hofmanova J, Hofer M, Znojil V, Minksova K, et al. The effect of nonsteroidal antiinflammatory drugs ibuprofen, flurbiprofen, and diclofenac on in vitro and in vivo growth of mouse fibrosarcoma. Cancer Invest 2002;20:490–8.
31. Boucher PD, Im MM, Freytag SO, Shewach DS. A novel mechanism of synergistic cytotoxicity with 5-fluorocytosine and ganciclovir in double suicide gene therapy. Cancer Res 2006;66:3230–7.
32. Haberland A, Schreiber S, Maia CS, Rübbelke MK, Schaller M, Korting HC, et al. The impact of skin viability on drug metabolism and permeation — BSA toxicity on primary keratinocytes. Toxicol In Vitro 2006;20:347–54.
33. Edelson RE, Gorycki PD, MacDonald TL. The mechanism of aphidicolin bioinactivation by rat liver in vitro systems. Xenobiotica 1990;20:273–87.
34. Vogt T, McClelland M, Jung B, Popova S, Bogenriede T, Becker B, et al. Progression and NSAID-induced apoptosis in malignant melanomas are independent of cyclooxygenase II. Melanoma Res 2001;11:587–99.
35. Rodriguez CO Jr, Mitchell BS, Ayres M, Eriksson S, Gandhi V. Arabinosylguanine is phosphorylated by both cytoplasmic deoxycytidine kinase and mitochondrial deoxyguanosine kinase. Cancer Res 2002;62:3100–5.
36. Baron JM, Holler D, Schiffer R, Frankenberg S, Neis M, Merk HF, et al. Expression of multiple cytochrome p450 enzymes and multidrug resistance-associated transport proteins in human skin keratinocytes. J Invest Dermatol 2001;116:541–8.
37. Schiffer R, Neis M, Holler D, Rodriguez F, Geier A, Gartung C, et al. Active influx transport is mediated by members of the organic anion transporting polypeptide family in human epidermal keratinocytes. J Invest Dermatol 2003;120:285–91.